Plant Cell, Tissue and Organ Culture (PCTOC) (2025) 162:82
https://doi.org/10.1007/s11240-025-03181-5

ORIGINAL ARTICLE

Impact of silver nanoparticles and silver nitrate on regeneration, biochemical traits, and nutrient composition of quinoa (*Chenopodium quinoa* willd.) in in vitro culture

Aras Türkoğlu[1] · Kamil Haliloğlu[2] · Ayşegül Kasapoğlu[3] · Damla Kızılkaya[3] · Barış Eren[4] · Fatih Demirel[4] · Muhammet İslam Işık[1] · Emre İlhan[3] · Hossein Abbasi Holasou[5] · Adem Güneş[6]

Received: 24 December 2024 / Accepted: 10 August 2025
© The Author(s), under exclusive licence to Springer Nature B.V. 2025

Abstract

Nanoparticles have proven effective in enhancing regeneration, morphological development, morpho physiology, and biochemical parameters of plantlets produced in vitro. This research aimed to examine the effects of silver nanoparticles (Ag-NPs) compared to silver nitrate ($AgNO_3$) on shoot organogenesis in the regeneration of quinoa (*Chenopodium quinoa* Willd.). To establish an efficient regeneration system the culture medium was then supplemented with $AgNO_3$ and Ag-NPs at a range of concentration, including 0, 2, 4, 6, and 8 mg L^{-1} of three types of explants (first node, middle node, and apical node). Ag-NPs yielded higher values than $AgNO_3$ across all measured parameters, including shoot length, callus count, leaf number, and shoot weight. A concentration of 6 mg L^{-1} produced the optimal results for these parameters, while 8 mg L^{-1} led to reduced growth, indicating a potential toxicity threshold. Apical node explants showed superior regeneration capacity across treatments. Biochemical analyses revealed increased antioxidant enzyme activity and malondialdehyde content under Ag treatments, suggesting oxidative stress, while hydrogen peroxide levels decreased, indicating enhanced reactive oxygen species scavenging at higher concentrations (4–8 mg L^{-1}). Our result showed the Ag treatments enhanced the uptake of phosphorus, potassium, and magnesium, while high concentrations resulted in decreased sodium and calcium levels, suggesting potential toxicity and impaired ion transport. Principal component analysis was employed to explore relationships among factors associated with tissue culture, revealing a strong association between high $AgNO_3$ concentrations, explant position, and shoot development. This study found that Ag-NPs significantly influenced the growth parameters and other traits of the plantlets. Furthermore, our results suggest that the efficiency of quinoa tissue culture can be enhanced by increasing the application of Ag in the form of nanoparticles. In conclusion, this work underscores the potential of using Ag-NPs in quinoa tissue culture.

Key message

Silver nanoparticles at optimal concentrations improve quinoa regeneration, morphology, antioxidant activity, and nutrient uptake in vitro, outperforming silver nitrate and offering potential for enhanced tissue culture protocols.

Keywords Quinoa · Nanoparticle · Shoot organogenesis

Introduction

Plant tissue culture methods, including plant regeneration through cell culture, somatic embryogenesis, and shoot organogenesis are fundamental to advancements in plant biotechnology and genetic engineering for plant improvement. Somatic embryogenesis (SE) allows for the regeneration of whole plants by harnessing the natural to first neoteny of cells (Sahrawat et al. 2003). This process can occur either through the conversion of pre-embryonic cells into somatic embryos or by the differentiation of established somatic tissue into a non-structural mass of proliferating cells, known

Communicated by Nhut Tan Duong.

Extended author information available on the last page of the article

Published online: 15 September 2025

as calli, from which somatic embryos can develop (Dosad and Chawla 2015; Rabha and Rout 2011). These two processes are referred to as direct and indirect somatic embryogenesis, respectively. In both cases, somatic embryos are typically derived from a small proportion of pre-embryonic or embryonically determined cells. As a result, the plant produced is the offspring of either a single cell or a small cluster of cells (Jiménez 2001; Mathew and Philip 2003). Often, initiating somatic embryogenesis requires the application of a single exogenous signal to a suitable explant. Auxins like naphthalene acetic acid (NAA) or 2,4-Dichlorophenoxyacetic acid (2,4-D) are commonly used for this purpose, though the process can also be triggered by other plant hormones or even macromolecules, such as certain (Ji et al. 2023; Pasternak and Steinmacher 2024). Vegetative propagation through in vitro cloning, facilitated by a controlled physical environment and a nutrient-rich medium, offers a reliable approach to achieving genetic uniformity in quinoa (Hesami and Daneshvar 2016). While shoot regeneration from organ and callus cultures is often associated with somaclonal variation, the use of shoot tip or meristem cultures enables the preservation of genetic fidelity in the propagated clones (Bhojwani and Dantu 2013).

Nanotechnology is one of the most exciting and rapidly advancing fields in modern science, offering innovative solutions by integrating various disciplines, including life sciences and materials engineering (Reddy et al. 2016). Applications of nanotechnology are found across a wide range of sectors, such as pesticide degradation and dispersion, creation of nano sensors, use of micronutrients in agriculture, and the protection and nutrition of plants (Ghormade et al. 2011). These applications suggest that nanoparticles (NPs) may play a pivotal role in driving innovation within agricultural systems. (Çığ et al. 2024). Despite the promise of nanotechnology is widely recognized, the question of how to optimize its use in agriculture to increase crop yields remains under debate. Among various nanomaterials Ag-NPs have gained significant attention due to their antibacterial properties and have been utilized in various applications, including reducing microbial contamination, inducing somaclonal variation, increasing proliferation rates, and producing bioactive compounds in vitro (Bello-Bello et al. 2018; Parzymies 2021; Pérez-Caselles et al. 2022; Rahmawati et al. 2022). Parallel to this, $AgNO_3$ is also known for its role as an ethylene action inhibitor, influencing in vitro tissue responses by modulating growth and morphogenesis (Cristea et al. 2012). For instance, the addition of $AgNO_3$ to culture media has been shown to enhance shoot development by effectively inhibiting ethylene production (Biddington 1992). Moreover, silver ions, particularly in nitrate form, are widely used in promoting somatic embryogenesis and organogenesis across different plant species due to their regulatory role in morphogenetic pathways (Cristea et al. 2012).

It is anticipated that advances in nanotechnology will be more effective when combined with compounds like silver nitrate ($AgNO_3$) and silver nanoparticles (Ag-NPs), as well as in vitro tissue culture techniques. In this context, several studies have shown that NPs can positively influence regeneration efficiency, morphological traits, morpho physiology, and biochemical responses in plantlets generated in vitro (Kulus and Tymoszuk 2021). However, while these substances offer substantial benefits, their effects are not universally positive. The impact of Ag-NPs, especially at higher concentrations, varies depending on factors such as plant species, developmental stage, and nanoparticle size and dosage (Vishwakarma et al. 2017). Some studies suggest that $AgNO_3$ acts as an inhibitor of ethylene action. Some studies have reported growth inhibition, reduced root length, and biomass accumulation under excessive Ag-NP exposure, highlighting potential phytotoxicity (Yin et al. 2011). Additionally, interactions between nanomaterials and plants have been shown to affect seed germination, root initiation, and growth, with these effects varying based on the properties, concentration of NPs, and the plant species involved (Lin and Xing 2007). The bioaccumulation of Ag-NPs within plant tissues has also been correlated with the system's redox potential, further complicating their use in plant systems (Haverkamp and Marshall 2009). Therefore, while both $AgNO_3$ and Ag-NPs exhibit promising effects on shoot and root development across various species (Khan et al. 2023; Yan and Chen 2019), caution is warranted regarding concentration-dependent toxicity. Interestingly, recent findings also point to the potential of NPs in facilitating genetic transformation, suggesting a new frontier in plant biotechnology (Wu et al. 2023). Despite increasing interest, there is still a notable gap in the literature regarding the effects of $AgNO_3$ and biosynthesized Ag-NPs on quinoa (*Chenopodium quinoa* Willd.) tissue culture. To address this research gap, the present study evaluates the regeneration efficiency, biochemical alterations, and nutrient composition resulting from the application of various concentrations of $AgNO_3$ and biosynthesized Ag-NPs across different types of explants of quinoa.

Materials and methods

Synthesis and characterization of silver nanoparticles (Ag-NPs)

In this study, Ag-NPs were synthesized using extracts from fresh *Eruca vesicaria* leaves (25 g) (Çiçek 2022). The leaves were washed 2–3 times with tap water to remove

dust and debris, followed by rinsing twice with distilled water to eliminate residual contaminants such as soil, insect waste, or microbes. After cleaning, the leaves were finely chopped and boiled with 200 mL of distilled water at 75 °C for a total of 15 min. The mixture was then cooled to room temperature and filtered using Whatman No. 1 filter paper to remove plant debris. The resulting extract was stored at 4 °C for use in nanoparticle synthesis. For the synthesis, 500 mL of 1 mM silver nitrate ($AgNO_3$) solution (Sigma-Aldrich, Cat. No. 7761–88-8, St. Louis, MO, USA) was prepared. Then, 10 mL of the *E. vesicaria* extract was added to the $AgNO_3$ solution. The reaction mixture was kept in a dark environment at room temperature to prevent photoactivation of silver ions. Within 1–2 min, a visible color change from colorless to reddish-brown occurred, indicating the reduction of Ag^+ ions to metallic silver (Ag°) and the formation of silver nanoparticles. This rapid color transition is a hallmark of successful nanoparticle synthesis via green methods. To purify the synthesized nanoparticles, the solution was centrifuged and washed at least three times with distilled water to remove unreacted plant compounds and other impurities. The final nanoparticle pellet was dried in an oven (Memmert UN110) at 75 °C. Characterization of the nanoparticles was performed using a UV–Vis spectrophotometer (Shimadzu, UV-3600 Plus, Kyoto, Japan), transmission electron microscopy (TEM) (Hitachi HighTech HT7700, Tokyo, Japan), and an X-ray diffractometer (XRD) (PANalytical, Empyrean, the Netherlands), following the methodology of a previous study (Çiçek 2022). A previous study (Çiçek 2022) reported that these Ag-NPs ranged in size from 5 to 20 nm and exhibited spherical, triangular, and cubic shapes, with absorption peaks observed at 250 and 450 nm. The nanoparticles also displayed a face-centered cubic crystal structure. Transmission Electron Microscopy (TEM), X-Ray Diffraction (XRD), and Fourier Transform Infrared Spectroscopy (FTIR) analyses of the relevant silver (Ag) nanomaterials are comprehensively presented in the study by Çiçek (2022).

In vitro conditions

The *Chenopodium quinoa* cultivar used in this study was the registered variety"Atlas". The seeds were initially washed under running tap water and subsequently surface-sterilized with 70% ethanol for 5 min. They were then treated with a 1% sodium hypochlorite solution containing a few drops of Tween-20 for 25 min under constant agitation. Following disinfection, the seeds were rinsed three times with sterile distilled water. The sterilized seeds were then imbibed in sterile distilled water for 24 h in the dark to facilitate hydration. Germination was conducted under dark conditions on hormone-free Murashige and Skoog (MS) medium (Murashige and Skoog 1962) supplemented with 20 g L^{-1} sucrose, 2 g L^{-1} phytagel, 1.95 g L^{-1} MES [2-(N-morpholino) ethanesulfonic acid], and distilled water. The pH of the medium was adjusted to 5.7–5.8 prior to autoclaving. Media containing basal MS salts and gelling agents were sterilized by autoclaving at 121 °C for 20 min. The seeds were incubated at 25 ± 1 °C for 14 days. Four different explant types were used for regeneration studies. On the eighth day of germination in hormone-free MS medium, explants were excised from the first, middle, and apical nodes of the seedlings. Ten explants were cultured in petri dishes containing MS medium supplemented with 20 g L^{-1} sucrose, 2 g L^{-1} phytagel, and one of five concentrations (0, 2, 4, 6, or 8 mg L^{-1}) of either silver $AgNO_3$ or biosynthesized Ag-NPs. Medium solidification, pH adjustment, and sterilization were performed as described previously. The explants were maintained in a controlled growth chamber at 25 ± 1 °C with a 16-h light (62 µmol m^{-2} s^{-1})/8-h dark photoperiod. For shoot regeneration, explants were cultured for 8 weeks on MS medium containing 1.0 mg L^{-1} BAP and the respective Ag treatments (Koçak et al. 2023). Subsequently, they were transferred to a root induction medium composed of MS salts supplemented with 0.5 mg L^{-1} BAP, again containing the same Ag treatments. Rooting cultures were maintained for 4 weeks under white fluorescent light (Preheat Daylight; 42 µmol photons m^{-2} s^{-1}) at 24 ± 1 °C with a 16-h photoperiod. The shoot length, number of calluses, number of leaves, and shoot weight were recorded after 30 days.

H_2O_2, MDA, and antioxidant enzyme activities (CAT, POD, and SOD)

At the end of the application period, hydrogen peroxide (H_2O_2) and malondialdehyde (MDA) contents two widely used indicators of oxidative stress and lipid peroxidation were determined according to the procedures of Tiryaki et al. (2019). H_2O_2 concentrations were expressed as µmol g^{-1} fresh weight (FW), while MDA contents were expressed as nmol g^{-1} fresh weight (FW). The activities of stress enzymes, including SOD, POD, and CAT, were assessed using a microplate reader (Multiskan GO, Thermo Scientific, Hudson, NH, USA) by absorbance measurements. SOD activity was determined by measuring the inhibition of NBT photoreduction. For each replicate, 20 µL of the sample, 170 µL of SOD assay buffer, and 10 µL of riboflavin solution were added to the wells of a spectrophotometer plate. Blank wells contained 190 µL of SOD assay buffer and 10 µL of riboflavin solution. The plate was incubated under fluorescent light for 10 min to develop the NBT color. It was then placed in the spectrophotometer, and absorbance was measured at 560 nm. One unit of SOD activity was defined as the enzyme amount causing 50% inhibition of

NBT reduction, with results expressed as U g^{-1} fresh leaf. For POD analysis, each replicate well was loaded with 5 µL of sample and 245 µL of POD assay buffer. Absorbance was recorded at 470 nm for 1 min at 15-s intervals. The amount of enzyme causing an absorbance increase of 0.01 in 1 min at 25 °C was defined as 1 unit, with results expressed as U g^{-1} fresh leaf. CAT activity was determined by measuring the decomposition rate of hydrogen peroxide (H_2O_2), which results in a decrease in absorbance at 240 nm. Each well received 20 µL of enzyme extract and 180 µL of CAT assay buffer containing H_2O_2. After 1 s of pre-shaking, the plate was read at 240 nm for 3 min at 30-s intervals. One unit of CAT activity was defined as the amount of enzyme required to degrade 1 µmol of H_2O_2 per minute under the assay conditions. Results were expressed as U g^{-1} fresh leaf tissue (Kaysım et al. 2024; Sahin et al. 2018).

Nutrient status

The mineral nutrient content of fresh quinoa leaves was determined following the method described by Mabotja et al. (2021), with slight modifications. Briefly, 0.5 g of fresh and ground leaf tissue was digested using a mixture of nitric acid (HNO_3) and hydrogen peroxide (H_2O_2) at a 2:3 (v/v) ratio. Digestion was performed in a microwave digestion system (Anton Paar Multiwave 7000) under a three-step temperature program: 5 min at 145 °C and 75% relative humidity, followed by 10 min at 180 °C and 90% relative humidity, and finally 10 min at 100 °C and 40% relative humidity. After digestion, samples were diluted appropriately, and elemental concentrations were determined using inductively coupled plasma optical emission spectrometry (ICP-OES; ICP-AES-9820, Shimadzu Corporation, Kyoto, Japan). The analyzed elements included macro- and micronutrients as well as trace elements: phosphorus (P), potassium (K), calcium (Ca), magnesium (Mg), sodium (Na), iron (Fe), copper (Cu), manganese (Mn), zinc (Zn), boron (B), chloride (Cl), and silver (Ag). Nutrient concentrations were expressed as mg kg^{-1}.

Table 1 Mean and variance analysis values of $AgNO_3$ and Ag-NPs at various concentration

Ag types	Shoot length (cm)	Callus number (number)	Leaf number (number)	Shoot weight (g)
$AgNO_3$	1.617[b1]	5.453[b]	8.187[b]	1.352[b]
Ag-NPs	2.820[a]	8.027[a]	13.760[a]	3.673[a]
Ag concentration (mg L^{-1})				
0	1.227[c]	6.133[c]	5.333[b]	1.073[e]
2	2.063[b]	5.000[d]	10.667[a]	2.182[d]
4	2.420[ab]	9.500[a]	12.467[a]	2.927[b]
6	2.803[a]	8.233[b]	13.800[a]	3.632[a]
8	2.580[a]	4.833[d]	12.600[a]	2.748[c]
Explant types				
Apical node	2.502[a]	7.620[a]	18.180[a]	3.352[a]
Middle node	2.096[b]	6.640[b]	7.780[b]	2.056[c]
First node	2.058[b]	5.960[c]	6.960[b]	2.129[b]
Mean square of Ag types	54.240[***2]	248.327[***]	1164.827[***]	201.956[***]
Mean square of Ag concentration	11.408[***]	126.590[***]	335.773[***]	27.453[***]
Mean square of explant types	3.028[**]	34.820[***]	1956.007[***]	26.506[***]

[1]Differences between means shown with the same lowercase letter in the same column for each application. [2]**significant at $p \leq 0.01$; ***significant at $p \leq 0.001$

Data analysis

The experiment was conducted using a factorial completely randomized design (CRD) with three factors: explant type (first node, middle node, and apical node), silver source ($AgNO_3$ and Ag-NPs), and five different concentrations (0, 2, 4, 6, and 8 mg L^{-1}). The experiments were set out in 10 replicates per treatment, and each treatment was repeated in three sets. Data were subjected to analysis of variance (ANOVA) using the General Linear Model (GLM) procedure in JMP statistical software (Version 15, SAS Institute Inc., Cary, NC, USA). Treatment means and their interactions were compared using the Duncan test at a 5% significance level. Principal component analysis (PCA) was performed using XLSTAT software (Addinsoft, New York, USA) to assess the relationships in vitro, biochemical and elemental contents measured under in vitro conditions.

Results

Effects of silver nitrate and silver nanoparticles on in vitro parameters

The analysis of variance revealed that types of silver source ($AgNO_3$ and Ag-NPs) had a statistically significant effect on all measured parameters. ANOVA for the concentrations of all parameters also showed statistical significance ($p \leq 0.001$). Additionally, the interaction between treatment and concentration yielded significant differences, with leaf number showing a statistically significant difference at $p \leq 0.01$, while all other parameters showed significance at $p \leq 0.001$ (Table 1). Table 1 shows the effects of $AgNO_3$ and Ag-NPs treatments on plant growth, as well as the role of different concentrations and plant explant types (apical node, intermediate, and first node) in these effects (Fig. 1). The results of the F-test (*** and **) confirm that all factors produced significant differences in the analyzed parameters, indicating that treatment, concentration, and explant type have a significant impact on plant growth. Ag-NPs yielded

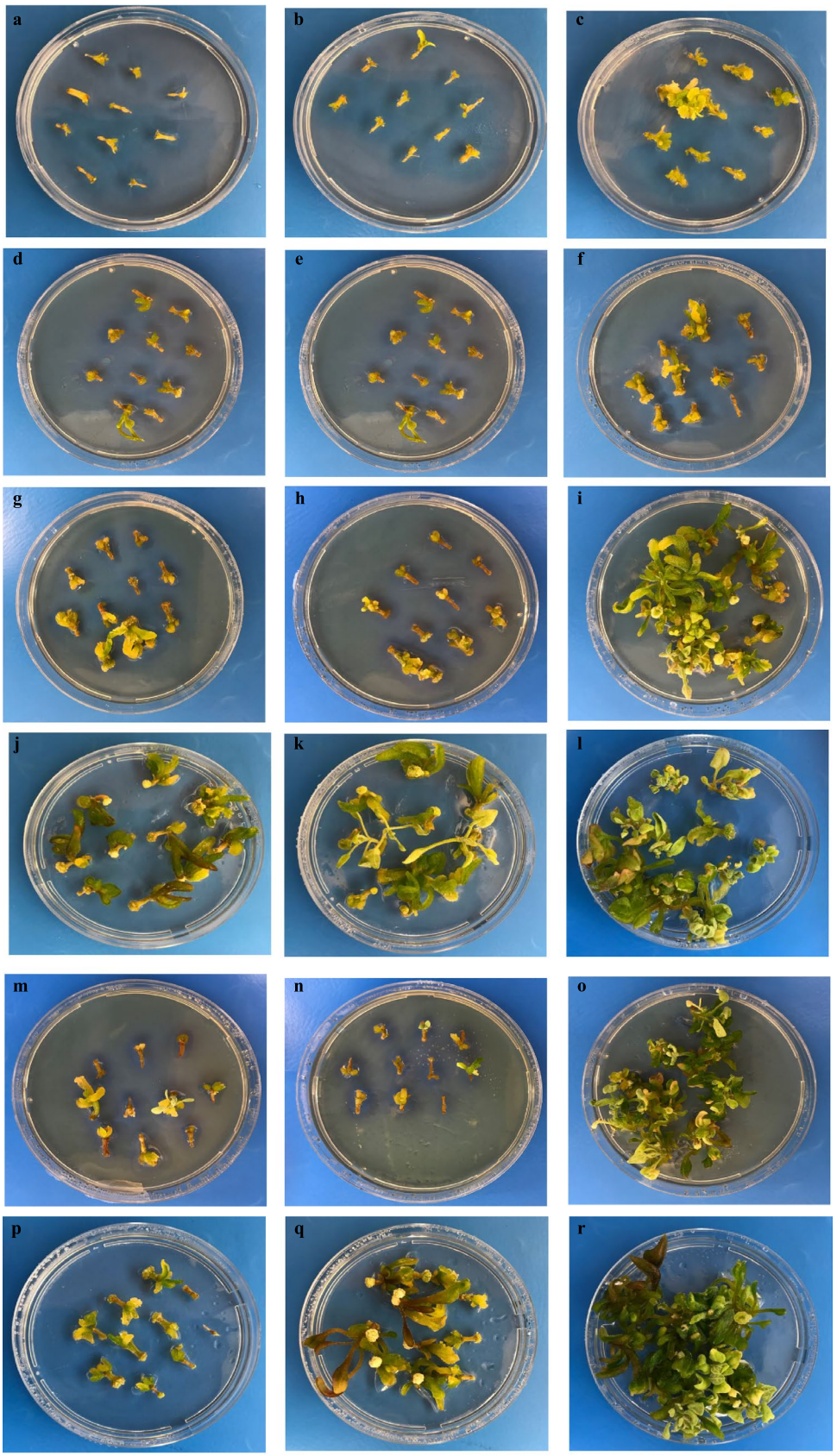

Fig. 1 Effects of different silver (Ag) sources and their concentrations on in vitro responses of various quinoa explants. Panels a–c represent the control groups without $AgNO_3$ and Ag-NPs treatment, showing the responses of first node (**a**), middle node (**b**), and apical node (**c**) explants, respectively. Panels d-f represent the 2 mg L^{-1} $AgNO_3$ treatment, showing the responses of first node (**d**), middle node (**e**), and apical node (**f**) explants, respectively. Panels g-h represent the 4 mg L^{-1} $AgNO_3$ treatment, showing the responses of first node (**g**), middle node (**h**), and apical node (**i**) explants, respectively. Panels j-k represent the 6 mg L^{-1} $AgNO_3$ treatment, showing the responses of first node (**j**), middle node (**k**), and apical node (**l**) explants, respectively. Panels m–o represent the 8 mg L^{-1} $AgNO_3$ treatment, showing the responses of first node (**m**), middle node (**n**), and apical node (**o**) explants, respectively. Panels p-r represent the 2 mg L^{-1} Ag-NPs treatment, showing the responses of first node (**p**), middle node (**q**), and apical node (**r**) explants, respectively. Panels s-u represent the 4 mg L^{-1} Ag-NPs treatment, showing the responses of first node (**s**), middle node (**t**), and apical node (**u**) explants, respectively. Panels v-x represent the 6 mg L^{-1} Ag-NPs treatment, showing the responses of first node (**d**), middle node (**e**), and apical node (**f**) explants, respectively. Panels y-aa represent the 8 mg L^{-1} Ag-NPs treatment, showing the responses of first node (**y**), middle node (**z**), and apical node (**aa**) explants, respectively

Fig. 1 (continued)

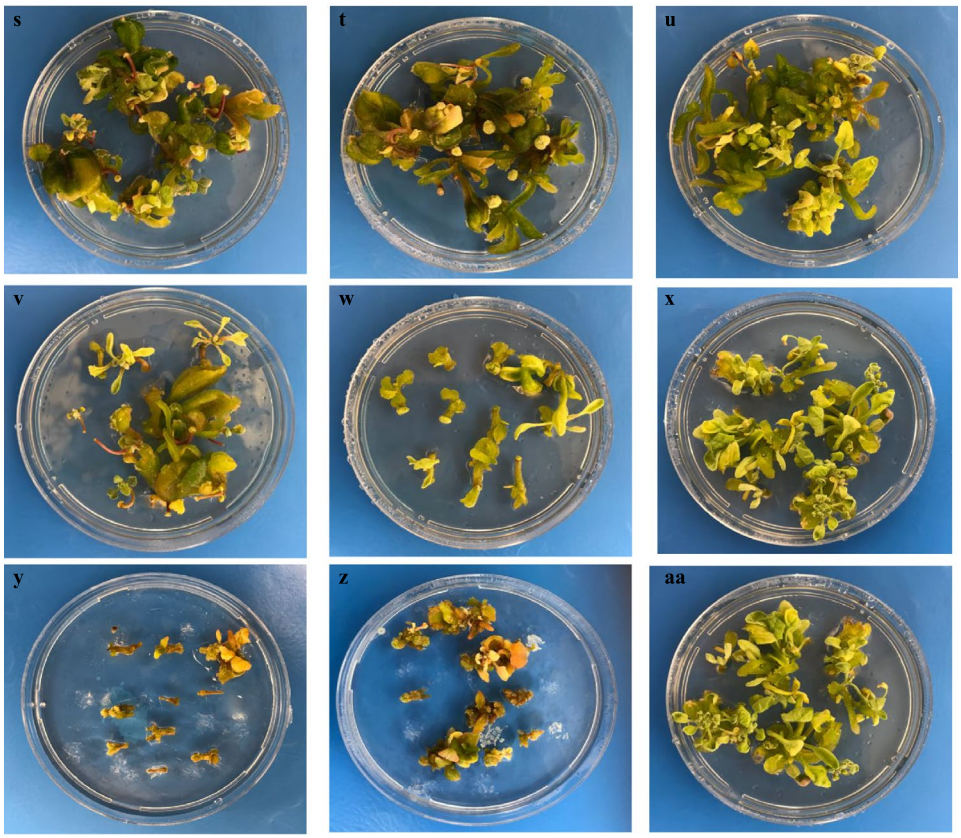

higher values than $AgNO_3$ across all parameters, including shoot length, callus number, leaf number, and shoot weight (2.820 cm, 8.027 number, 13.760 number, 3.673 g). In general, a concentration of 6 mg L^{-1} produced the best results in shoot length, callus number, leaf number, and shoot weight (2.803 cm, 8.233 number, 13.800 number, 3.632 g), while higher concentrations (8 mg L^{-1}) resulted in a decline in some parameters, suggesting potential phytotoxic effects. Apical node explants exhibited the highest values for plant growth and development compared to other explant types, indicating that apical node explants may be more effective in supporting plant regeneration (Table 1).

According to Table 1, the highest shoot length was 2.803 cm with the 6 mg L^{-1} Ag-NPs treatment, while the lowest was 1.227 cm at the 0 mg L^{-1} concentration. This suggests that Ag-NPs promoted greater shoot length compared to $AgNO_3$, and medium-to-high concentrations favored shoot development. The highest callus number was 9.500 number at the 4 mg L^{-1} Ag-NPs treatment, while the lowest was 5.000 number at the 2 mg L^{-1} concentration, indicating that 4 mg L^{-1} Ag-NPs treatment enhanced cell division and callus formation more effectively. The highest leaf number was 18.180 in the apical node explant type, while the lowest was 6.960 number in the first node explant type, indicating that apical node explants were more effective in promoting leaf formation. The highest shoot weight was 3.632 g with the 6 mg L-1 Ag concentration, while the lowest was 1.073 g at the 0 mg L-1 concentration. Additionally, it was determined that Ag-NPs treatment (3.673 g) increased shoot weight compared to $AgNO_3$ (1.352 gr).

The results in Table S1 show the effects of Ag types and Ag concentration interaction, Ag types and explant types interaction, Ag concentration and explant types interaction on plant growth parameters. According to the ANOVA results, the interaction between Ag types and Ag concentrations was found to be statistically significant for all measured traits ($p \leq 0.001$ or $p \leq 0.01$). The interaction between Ag types and explant types showed significant effects on shoot length ($p \leq 0.05$), callus number ($p \leq 0.001$), and shoot weight ($p \leq 0.001$). Furthermore, the interaction between Ag concentrations and explant types was also statistically significant for shoot length ($p \leq 0.05$), callus number ($p \leq 0.001$), and shoot weight ($p \leq 0.001$). Notably, treatment with Ag-NPs at 6 mg L^{-1} resulted in the highest shoot length (3.653 cm), shoot weight (5.490 g), number of leaves (18.33), and substantial callus number (9.33), indicating superior performance across all traits. This was followed by Ag-NPs at 8 mg L^{-1} and 4 mg L^{-1}, which also produced high leaf numbers (above 14) and shoot weights exceeding 3.7 g. In contrast, $AgNO_3$ treatments generally yielded lower morphological values, with 2 mg L^{-1} showing the lowest shoot length, leaf number, and shoot weight among

all treatments. Control groups (0 mg L^{-1}), for both $AgNO_3$ and Ag-NPs, exhibited comparable outcomes, ranking among the lowest in terms of shoot development and biomass accumulation. These findings clearly demonstrate that Ag-NPs are more bio-effective than $AgNO_3$ and, at optimal concentrations particularly 6 mg L^{-1} significantly promote shoot growth and organogenesis in quinoa explants (Fig. 2).

The three-way interaction among silver type, concentration, and explant type revealed statistically significant effects on shoot length, callus number, and shoot weight, as indicated by ANOVA ($p \leq 0.05$ for shoot length, $p \leq 0.001$ for callus number and shoot weight) (Table S2). The most notable morphogenic responses were obtained from treatments combining Ag-NPs at 6 mg L^{-1} with first node and apical node explants, producing the highest values across all traits: shoot length (4.080 cm), callus number (10.000), shoot weight (6.500 g), and a leaf number of 25.4. Ag-NPs generally outperformed $AgNO_3$ at corresponding concentrations across all explants, especially at moderate doses (2–6 mg L^{-1}). Conversely, low concentrations of $AgNO_3$ (e.g., 2 mg L^{-1}) showed minimal or no callus formation and poor shoot development, particularly in middle and first node explants. These findings underscore the superior efficacy of Ag-NPs in stimulating shoot organogenesis and biomass accumulation in quinoa, particularly when combined with apical or first node explants at 6 mg L^{-1}, while also highlighting the limited regenerative capacity under $AgNO_3$ treatments or in middle node explants at low doses (Fig. 3).

Biochemical measurements

The analysis of variance indicated that all main effects Ag type, concentration, and explant type had statistically significant influences on all five biochemical parameters (CAT, POD, SOD, MDA, and H_2O_2) at $p \leq 0.001$ (Table 2). Among Ag treatments, Ag-NPs significantly enhanced CAT, POD, and MDA levels compared to $AgNO_3$, while reducing H_2O_2 accumulation. Although SOD values were numerically close, a small but significant difference was detected ($AgNO_3$ > Ag-NPs). As Ag concentration increased from 0 to 8 mg L^{-1}, a progressive and significant elevation was observed in CAT, POD, and MDA activities, with maximum CAT (16.234), POD (35.622), and MDA (0.412) at 8 mg L^{-1}. Conversely, H_2O_2 levels declined sharply, with the lowest value (0.153) at 8 mg L^{-1}, indicating enhanced oxidative stress mitigation. SOD activity peaked at 6 mg L^{-1} (19.173). Regarding explant type, first node explants exhibited the highest CAT, POD, and SOD activities, followed by apical and middle nodes. MDA content was highest in apical explants, suggesting higher lipid peroxidation, while middle nodes showed the lowest H_2O_2 and MDA levels, reflecting comparatively lower oxidative damage. Collectively, the data emphasize the superior performance of Ag-NPs and higher concentrations (6–8 mg L^{-1}) in enhancing antioxidant enzyme activity and reducing oxidative stress indicators in quinoa explants.

The two-way interaction effects between silver (Ag) types, Ag concentrations, and explant types exhibited statistically significant differences for all measured biochemical parameters (CAT, POD, SOD, MDA, and H_2O_2) ($p \leq 0.001$) (Table S3). Among the Ag type × concentration interactions, the combination of Ag-NPs with 8 mg L^{-1} resulted in the highest CAT activity (16.937 EU g^{-1}) and among the highest SOD values (19.143 EU g^{-1}), indicating an enhanced antioxidant defense. The $AgNO_3$ × 0 mg L^{-1} and Ag-NPs × 0 mg L^{-1} treatments showed the lowest CAT (14.407 EU g^{-1}) and SOD values, reflecting baseline activity in the absence of silver treatment. In terms of POD activity, the most pronounced interaction was observed for Ag-NPs × 4 mg L^{-1} (35.923 EU g^{-1}), while the lowest was for $AgNO_3$ × 0 mg L^{-1} (30.993 EU g^{-1}), indicating that both the silver form and concentration substantially in

fluence peroxidase response. The MDA content, indicative of lipid peroxidation, was lowest in the $AgNO_3$ × 2 mg L^{-1} treatment (0.347 nmol g^{-1}), suggesting reduced oxidative stress at lower $AgNO_3$ concentrations. In contrast, Ag-NPs × 2 mg L^{-1} and Ag-NPs × 8 mg L^{-1} yielded the highest MDA values (0.413 nmol g^{-1}), possibly reflecting a dose-dependent pro-oxidant effect at certain nanoparticle concentrations. For H_2O_2 content, the interaction effect revealed that Ag-NPs × 2 mg L^{-1} resulted in the lowest accumulation (0.140), supporting the role of Ag-NPs in ROS scavenging. The highest H_2O_2 level (0.237 mmol kg^{-1}) was observed in $AgNO_3$ × 0 mg L^{-1} and Ag-NPs × 0 mg L^{-1}, serving as control benchmarks. Regarding the Ag type × explant type interaction, Ag-NPs × apical node yielded the highest CAT (16.102 EU g^{-1}) and MDA (0.426 nmol g^{-1}), while $AgNO_3$ × middle node generally resulted in lower CAT and SOD values. This suggests that both the source of Ag and the explant region collectively modulate oxidative responses. In the Ag concentration × explant type interaction, first node explants at 8 mg L^{-1} exhibited the highest CAT activity (16.300 EU g^{-1}) and relatively elevated SOD and POD values, whereas the lowest antioxidant activities were recorded in the untreated middle and first node explants. This underscores a synergistic effect of explant physiology and Ag dose on biochemical stress modulation (Fig. 4).

The three-way interaction among silver type, silver concentration, and explant type revealed statistically significant effects on all evaluated biochemical parameters (CAT, POD, SOD, MDA, and H_2O_2) ($p \leq 0.001$) (Table S4). These results indicate that the antioxidant and oxidative stress responses in plant tissue are highly dependent on the combined influence of Ag source, dosage, and tissue origin. For CAT activity,

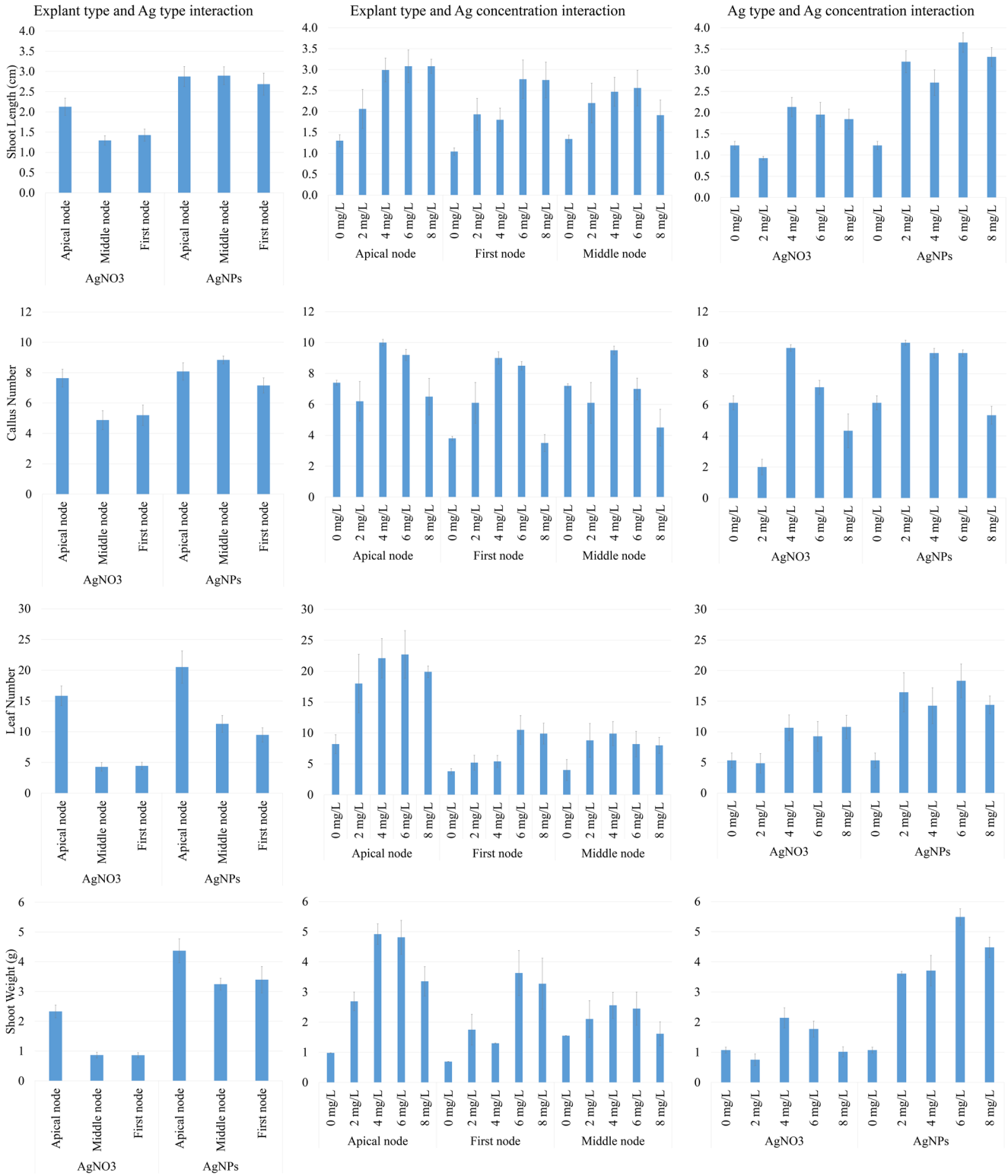

Fig. 2 Interactive effects of explant type, Ag type, and Ag concentration on morphological parameters in in vitro culture

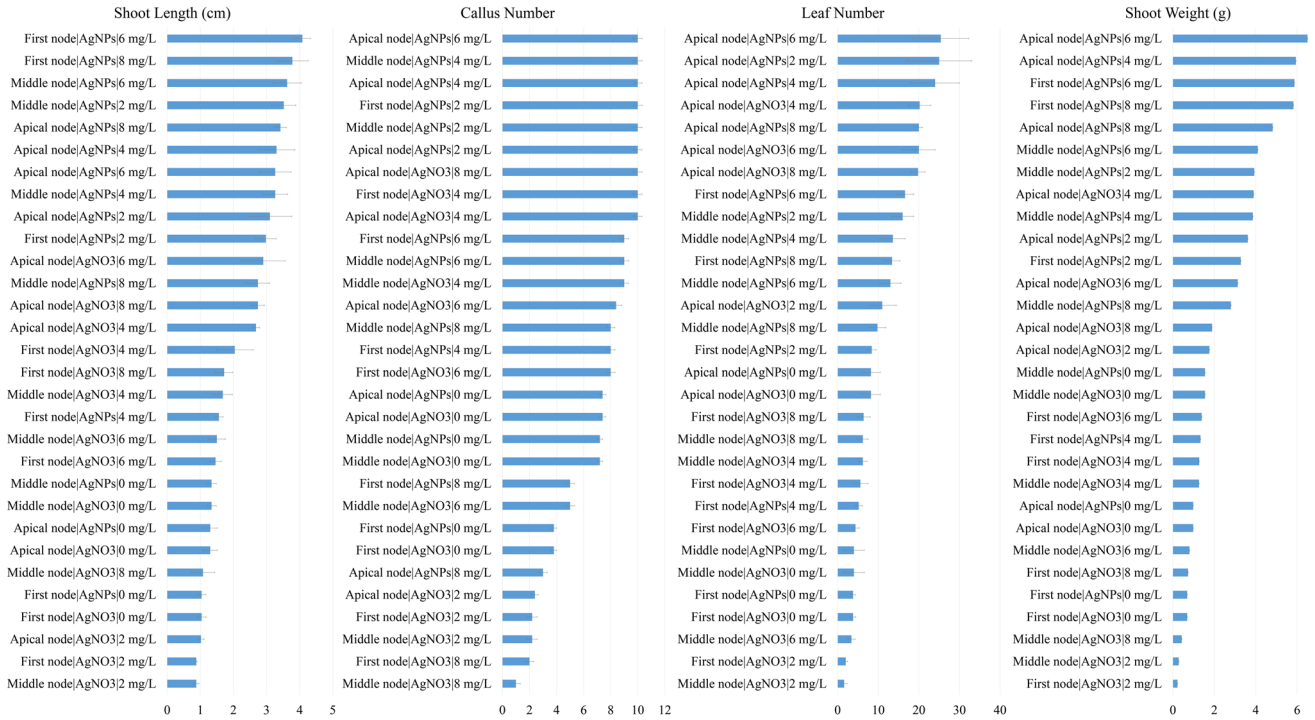

Fig. 3 Influence of Ag type × concentration × explant source interactions on morphogenic traits under in vitro conditions

Table 2 Mean and analysis of variance values of CAT, POD, SOD, MDA, and H_2O_2 of $AgNO_3$ and Ag-NPs

Ag types	CAT (EU g−1)	POD (EU g−1)	SOD (EU g−1)	MDA (nmol g−1) DW	H_2O_2 (mmol kg^{-1})
$AgNO_3$	15.113[b1]	33.703[b]	18.678[a]	0.378[b]	0.189[a]
Ag-NPs	15.931[a]	34.493[a]	18.669[b]	0.395[a]	0.170[b]
Ag concentration (mg L^{-1})					
0	14.407[e]	30.993[e]	18.253[e]	0.357[d]	0.237[a]
2	15.525[d]	33.813[d]	18.457[c]	0.380[c]	0.170[c]
4	15.583[c]	35.622[a]	18.408[d]	0.380[c]	0.175[b]
6	15.862[b]	35.005[c]	19.173[a]	0.403[b]	0.162[d]
8	16.234[a]	35.057[b]	19.075[b]	0.412[a]	0.153[e]
Explant types					
Apical node	15.510[b]	33.630[c]	18.832[b]	0.405[a]	0.182[a]
Middle node	15.390[c]	34.078[b]	18.323[c]	0.365[c]	0.175[c]
First node	15.667[a]	34.586[a]	18.865[a]	0.389[b]	0.181[b]
Mean square of Ag types	15.063[***2]	14.019[***]	0.002[***]	0.006[***]	0.008[***]
Mean square of Ag concentration	8.418[***]	62.025[***]	3.172[***]	0.009[***]	0.020[***]
Mean square of explant types	0.580[***]	6.864[***]	2.770[***]	0.012[***]	0.000[***]

[1]Differences between means shown with the same lowercase letter in the same column for each application. ***significant at $p \leq 0.001$

the highest value (17.40) was observed in explants treated with Ag-NPs at 6 mg L^{-1} on apical nodes, followed closely by Ag-NPs at 8 mg L^{-1} on middle (17.21 EU g^{-1}) and first nodes (16.90 EU g^{-1}). In contrast, the lowest CAT values (14.33 EU g^{-1}) were recorded in untreated apical explants of both $AgNO_3$ and Ag-NP treatments, indicating a substantial CAT enhancement due to Ag-NPs at moderate-to-high concentrations. Regarding POD activity, Ag-NPs at 6 mg L^{-1} on middle nodes induced the highest POD level (36.70 EU g^{-1}), suggesting a strong peroxidative response in that condition. Conversely, the lowest POD values (~30.22–30.54) were consistently observed in untreated middle and first nodes under both silver forms, emphasizing the elicitor role of Ag treatments. SOD activity peaked (19.70 EU g^{-1}) in $AgNO_3$ at 6 mg L^{-1} on apical nodes, reflecting a robust enzymatic defense in response to oxidative stress. Other combinations, such as Ag-NPs at 8 mg L^{-1} on middle nodes (19.45), also displayed high SOD levels. In contrast, lowest SOD values (17.65 EU g^{-1}) were observed in untreated middle nodes under both silver treatments. In terms of MDA content, which reflects lipid peroxidation, the highest value (0.48 nmol g^{-1}) was detected in Ag-NPs at 2 mg L^{-1} on apical nodes, potentially suggesting oxidative damage at this concentration. On the other hand, the lowest MDA levels (0.28–0.30 nmol g^{-1}) were noted in $AgNO_3$ at 2 mg L^{-1} on apical and first nodes, indicating a protective effect at lower $AgNO_3$ doses. Finally, H_2O_2 content was greatest (0.250 mmol kg^{-1}) in untreated apical explants, while the lowest



Fig. 4 Influence of two-way interactions between Ag type, concentration, and explant type on biochemical parameters in in vitro cultures

H_2O_2 levels (0.130–0.140 mmol kg^{-1}) were observed in Ag-NPs at 2 mg L^{-1} on apical and middle nodes, highlighting the potential of Ag-NPs at moderate levels in minimizing ROS accumulation (Fig. 5). In summary, this three-way interaction demonstrates that Ag-NPs generally promoted higher antioxidant enzyme activities and reduced oxidative markers compared to $AgNO_3$, particularly when applied at 6–8 mg L^{-1}. Moreover, apical and first node explants responded more dynamically to Ag treatments than middle nodes, underlining the importance of explant source in modulating stress physiology.

Effect of $AgNO_3$ and Ag-NPs on nutrient status

Analysis of variance indicated that the silver treatment type, concentration, and explant origin had significant effects on the uptake and accumulation of various macroelements phosphorus (P), potassium (K), calcium (Ca), magnesium (Mg), and sodium (Na) and microelements iron (Fe), copper (Cu), manganese (Mn), zinc (Zn), boron (B), chlorine (Cl), and silver (Ag) in plant tissues ($p \leq 0.001$ for most parameters) (Table 3).

Silver nanoparticles (Ag-NPs) significantly enhanced the accumulation of Ca, Mg, Fe, Cu, Mn, Zn, Cl, and Ag compared to $AgNO_3$, while $AgNO_3$ treatment resulted in higher P, K, and Na levels. Notably, Ag-NPs treatment led to a marked increase in Fe (22.623 vs. 21.851), Mn (10.917 vs. 10.372), Zn (8.029 vs. 7.397), and Ag (0.061 vs. 0.053) concentrations relative to $AgNO_3$, suggesting a more pronounced effect of nanoparticle-based silver in promoting the uptake of several essential and non-essential elements. Concentration-dependent effects were prominent across most elements. The 4 mg L^{-1} treatment generally resulted in the highest accumulation of P (416.500), Ca (661.500), and Mg (312.500), whereas 8 mg L^{-1} promoted the highest Ag accumulation (0.067). Interestingly, Na content decreased consistently with increasing Ag concentrations. Explant origin also played a significant role. The first node tissues exhibited the highest concentrations of Ca (617.800), Cu (11.503), Fe (22.859), Zn (7.788), Cl (0.031), and Ag (0.059), indicating that this region may have a higher capacity for elemental accumulation, possibly due to greater metabolic activity or vascular connectivity. In contrast, middle node tissues showed the highest P (377.500) and Na (133.800) levels. Collectively, these findings demonstrate that Ag-NPs at moderate-to-high concentrations (4–8 mg L^{-1}) can significantly alter nutrient uptake profiles and enhance the accumulation of several key elements, while the choice of explant type (particularly first node) further modulates this response, underscoring the complex interaction between nanomaterial exposure and plant physiology.

The two-way interaction effects among silver types, concentrations, and explant types revealed statistically significant differences ($p \leq 0.001$) Across all examined macro- and microelements, including P, K, Ca, Mg, Na, Fe, Cu, Mn, Zn, B, Cl, and Ag accumulation. (Table S5). Specifically, the

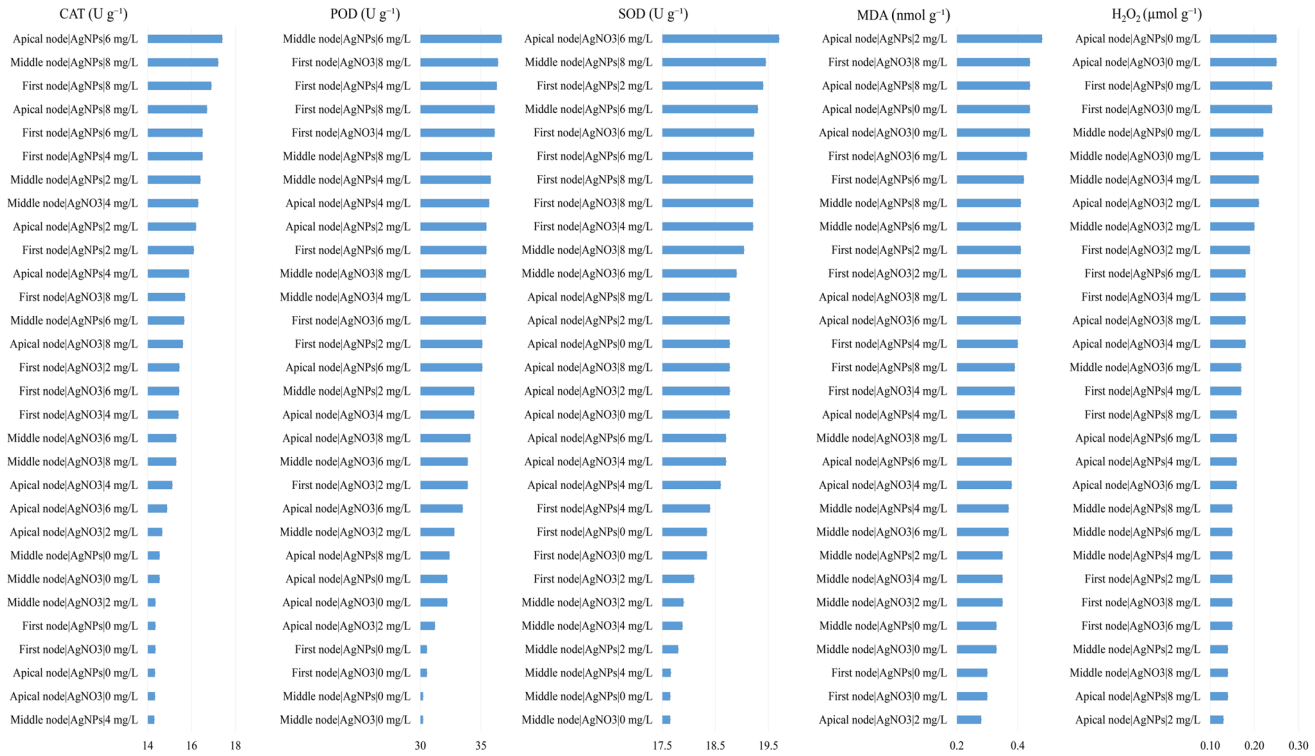

Fig. 5 Three-way interaction effects of Ag type, Ag concentration, and explant type on antioxidant enzyme activities and oxidative stress indicators

Table 3 Mean and analysis of variance values of $AgNO_3$ and Ag-NPs on nutrient status

Ag types	P (mg kg^{-1})	K (mg kg^{-1})	Ca (mg kg^{-1})	Mg (mg kg^{-1})	Na (mg kg^{-1})	Fe (mg kg^{-1})	Cu (mg kg^{-1})	Mn (mg kg^{-1})	Zn (mg kg^{-1})	B (mg kg^{-1})	Cl (mg kg^{-1})	Ag (mg kg^{-1})
$AgNO_3$	380.600^{a}[1]	1404.600^{a}	602.600^{b}	281.133^{b}	139.200^{a}	21.851^{b}	11.294^{b}	10.372^{b}	7.397^{b}	1.717^{a}	0.027^{b}	0.053^{b}
Ag-NPs	373.244^{b}	1363.267^{b}	626.000^{a}	298.733^{a}	124.200^{b}	22.623^{a}	11.417^{a}	10.917^{a}	8.029^{a}	1.697^{b}	0.029^{a}	0.061^{a}
Concentration (mg L^{-1})												
0	353.333^{e}	1299.667^{e}	552.667^{e}	228.667^{e}	160.000^{a}	18.913^{e}	11.087^{e}	9.823^{e}	7.180^{e}	1.557^{e}	0.027^{c}	0.033^{e}
2	375.778^{b}	1368.167^{d}	610.000^{c}	296.167^{d}	131.667^{c}	22.022^{d}	11.187^{d}	10.732^{c}	7.713^{c}	1.608^{d}	0.030^{b}	0.063^{b}
4	416.500^{a}	1406.500^{b}	661.500^{a}	312.500^{a}	133.333^{b}	22.847^{c}	11.668^{a}	10.610^{d}	7.872^{b}	1.748^{c}	0.027^{c}	0.062^{c}
6	366.333^{d}	1448.667^{a}	646.667^{b}	308.333^{b}	119.667^{d}	23.065^{b}	11.503^{b}	11.145^{a}	7.568^{d}	1.813^{a}	0.025^{d}	0.060^{d}
8	372.667^{c}	1396.667^{c}	600.667^{d}	304.000^{c}	113.833^{e}	24.338^{a}	11.332^{c}	10.913^{b}	8.230^{a}	1.808^{b}	0.032^{a}	0.067^{a}
Explant types types												
Apical node	376.567^{b}	1370.400^{c}	602.400^{c}	294.100^{a}	128.900^{c}	21.558^{c}	11.392^{b}	10.765^{a}	7.628^{c}	1.681^{c}	0.024^{c}	0.053^{b}
Middle node	377.500^{a}	1378.600^{b}	622.700^{a}	290.800^{b}	133.800^{a}	22.294^{b}	11.171^{c}	10.659^{b}	7.722^{b}	1.713^{b}	0.029^{b}	0.059^{a}
First node	376.700^{b}	1402.800^{a}	617.800^{b}	284.900^{c}	132.400^{b}	22.859^{a}	11.503^{a}	10.510^{c}	7.788^{a}	1.727^{a}	0.031^{a}	0.059^{a}
Treatment	1217.344^{***}[2]	$38,440.000^{***}$	$12,320.100^{***}$	6969.600^{***}	5062.500^{***}	13.386^{***}	0.339^{***}	6.691^{***}	8.987^{***}	0.008^{***}	0.000^{***}	0.002^{***}
Concentration	$10,144.711^{***}$	$54,950.650^{***}$	$32,753.100^{***}$	$21,771.650^{***}$	5704.100^{***}	74.547^{***}	0.995^{***}	4.526^{***}	2.689^{***}	0.250^{***}	0.000^{**}*	0.003^{***}
ExplantTypes	7.644^{*}	8513.200^{***}	3366.300^{***}	651.700^{***}	191.100^{***}	12.768^{***}	0.857^{***}	0.492^{***}	0.194^{***}	0.017^{***}	0.000^{***}	0.000^{***}

[1]Differences between means shown with the same lowercase letter in the same column for each application. [2]*significant at $p \leq 0.05$; ***significant at $p \leq 0.001$

combination of Ag-NPs at 4 mg L^{-1} resulted in the highest values for P (421.33 mg kg^{-1}), Ca (690.00 mg kg^{-1}), and Zn (8.417 mg kg^{-1}), while Ag-NPs at 8 mg L^{-1} yielded the greatest Ag content (0.067 mg kg^{-1}), suggesting a dose-dependent enhancement in nutrient uptake by Ag-NPs compared to $AgNO_3$. Among explant types, the first node under Ag-NPs treatment consistently exhibited superior elemental accumulation, especially for Ag (0.066 mg kg^{-1}), Zn (7.964 mg kg^{-1}), and Fe (23.408 mg kg^{-1}), indicating its enhanced physiological responsiveness and ion transport capacity. Regarding the concentration × explant interaction, the highest elemental concentrations were often recorded in first node explants exposed to intermediate Ag-NPs doses (4–6 mg L^{-1}), notably for Ca (669.00 mg kg^{-1} at 6 mg L^{-1}) and Zn (8.500 mg kg^{-1} at 8 mg L^{-1} middle node). The interaction between Ag type and explant type was also significant, with Ag-NPs × first node combinations yielding the highest values for most parameters. These results collectively emphasize that both the form of silver and the explant tissue type critically influence the elemental composition of regenerated tissues, with Ag-NPs and basal explants (first nodes) offering the most favorable outcomes for nutrient uptake and silver bioaccumulation (Figs. 6, 7).

The three-way interaction among Ag type, Ag concentration, and explant type had a statistically significant effect on all macro- and microelement contents ($p \leq 0.001$), as evidenced by the ANOVA results (Table S6). The elemental accumulation patterns varied distinctly across combinations, highlighting complex interdependencies. Notably, P reached its maximum value (432.000 mg kg^{-1}) in the Ag-NPs × 4 mg L^{-1} × first node treatment, while K peaked (1512.000 mg kg^{-1}) under $AgNO_3$ × 6 mg L^{-1} × middle node. Ca content was highest (712.000 mg kg^{-1}) in the Ag-NPs × 4 mg L^{-1} × middle node group. Mg and Na exhibited optimal uptake (344.000 mg kg^{-1} and 166.000 mg kg^{-1}, respectively) in Ag-NPs × 4 mg L^{-1} × middle node and $AgNO_3$ × 0 mg L^{-1} × middle node, demonstrating tissue-specific and concentration-sensitive responses. Among micronutrients, Fe content was maximized (25.440 mg kg^{-1}) in $AgNO_3$ × 8 mg L^{-1} × first node, while Cu reached 12.990 mg kg^{-1} under $AgNO_3$ × 8 mg L^{-1} × middle node. Mn peaked at 12.330 mg kg^{-1} in Ag-NPs × 6 mg L^{-1} × apical node, and Zn was most abundant (9.120 mg kg^{-1}) in Ag-NPs × 8 mg L^{-1} × middle node. Ag accumulation also exhibited significant interaction effects, with the highest content (0.090 mg kg^{-1}) observed in Ag-NPs × 2 mg L^{-1} × first node, suggesting efficient silver ion uptake and bioavailability in this combination. These results demonstrate that not only the type and concentration of silver but also the explant origin substantially influence nutrient and silver absorption. First node explants under Ag-NPs treatments at moderate concentrations (2–4 mg L^{-1}) generally provided superior outcomes, suggesting their

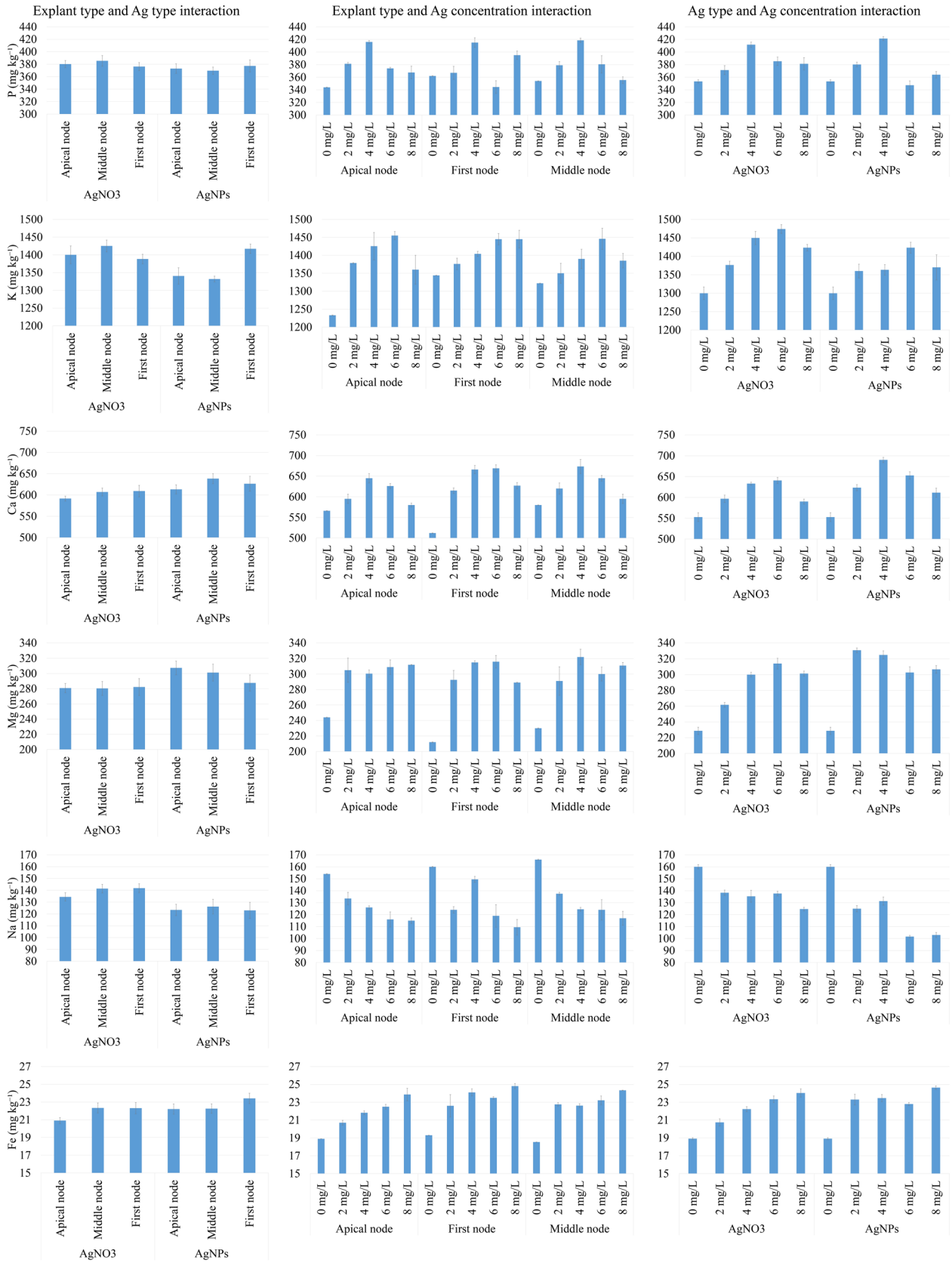

Fig. 6 Two-way interaction effects of Ag type, Ag concentration, and explant type on macro- and micronutrient content in explants

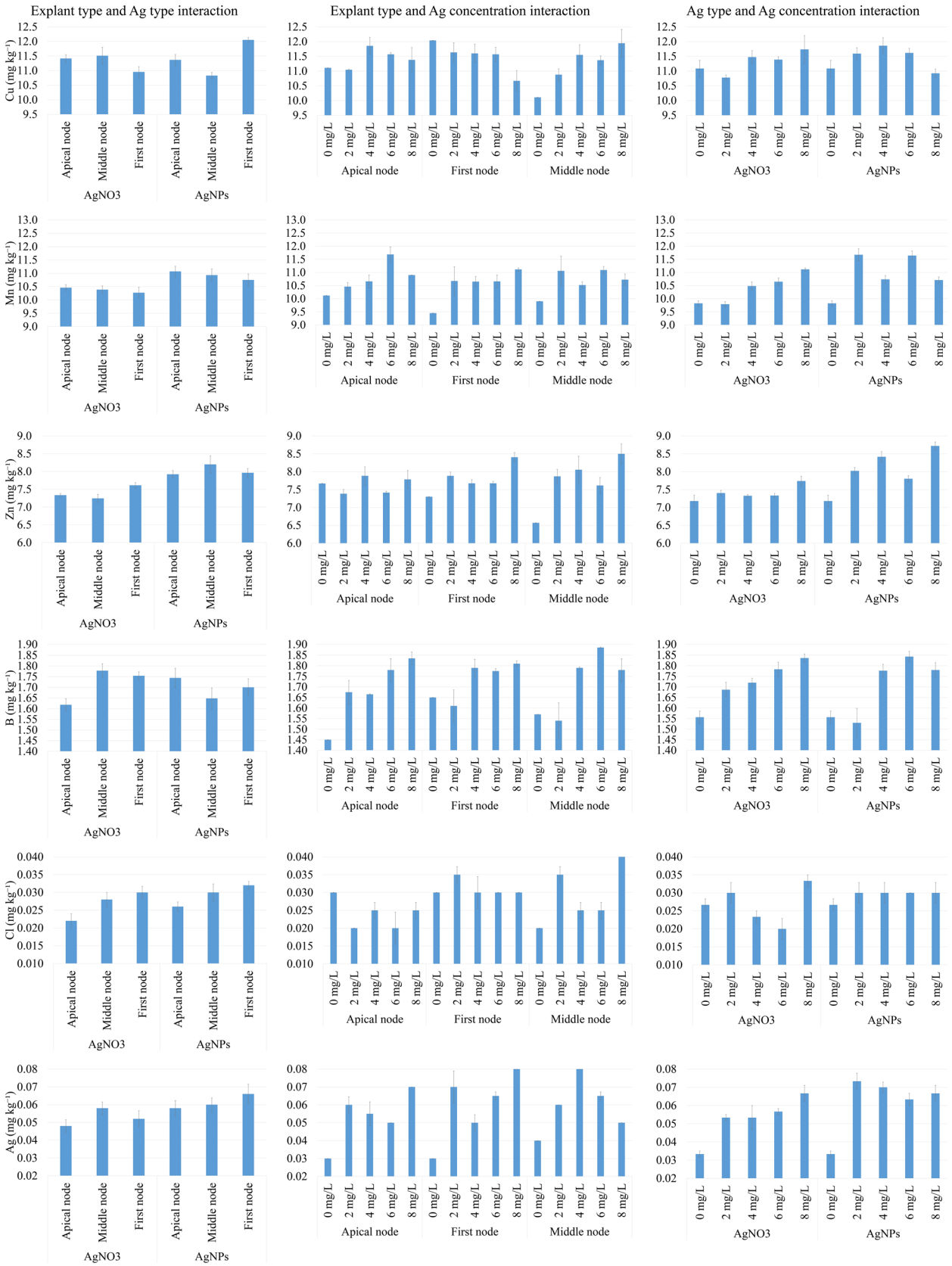

Fig. 7 Two-way interaction effects of Ag type, Ag concentration, and explant type on micronutrient uptake and silver accumulation in explants

higher metabolic activity and transport efficiency under nanomaterial exposure (Figs. 8, 9).

Principal component analysis

According to the first two main components (F1 and F2). which together explain 92.23% of the total variance. Figure 10 is a binary plot that illustrates the distribution of treatments (S1 to S30) based on the data. In this study. the treatments are grouped together along these primary components. demonstrating how their responses differ based on the quantities of $AgNO_3$ and Ag-NPs as well as the placements of the explants (apical node. middle node. and first node). For the variables"shoot length""leaf number."and"shoot

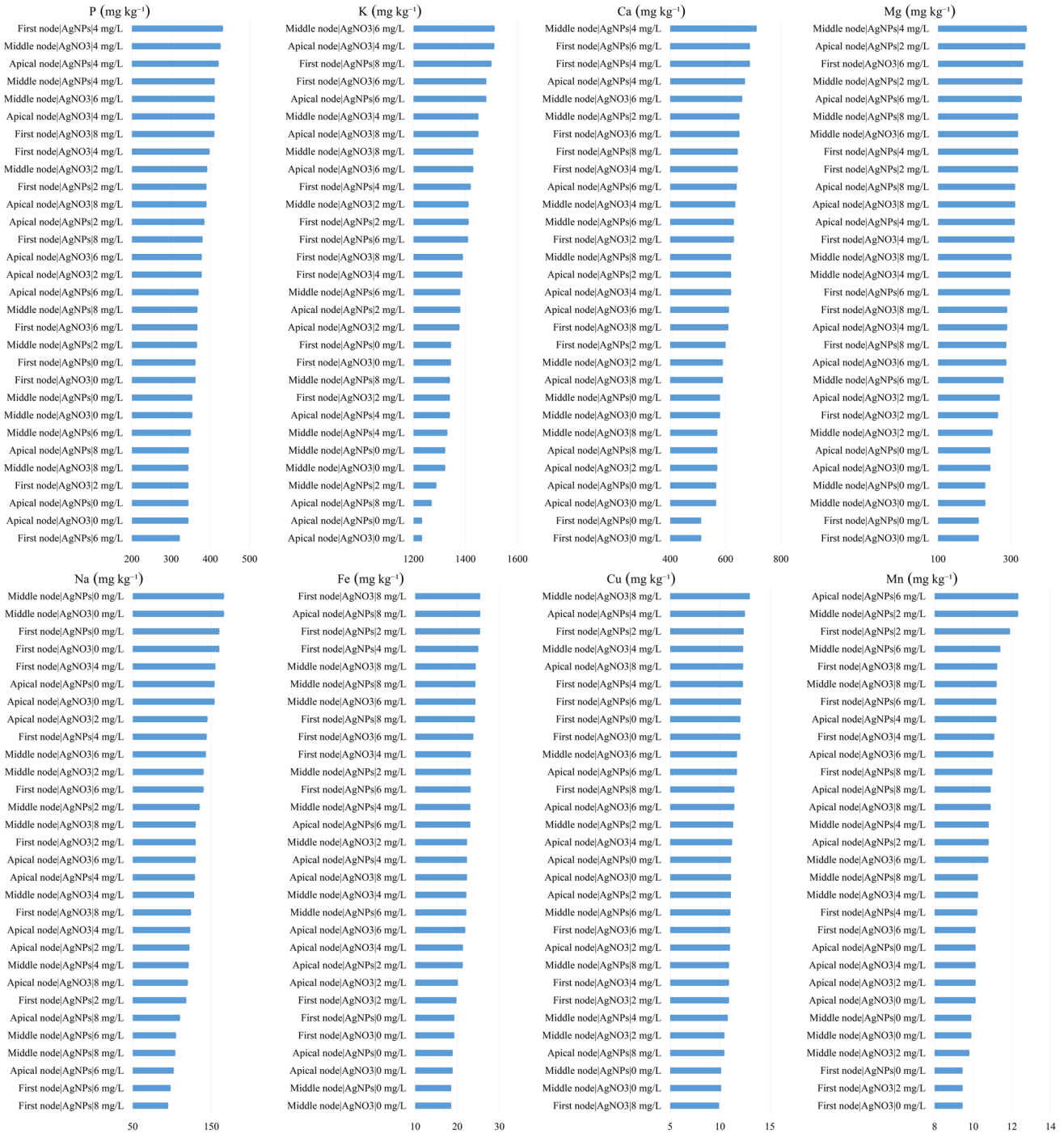

Fig. 8 Three-way interaction effects of explant type, silver source ($AgNO_3$ and Ag-NPs), and Ag concentration on macro- and micronutrient accumulation in in vitro cultured tissues

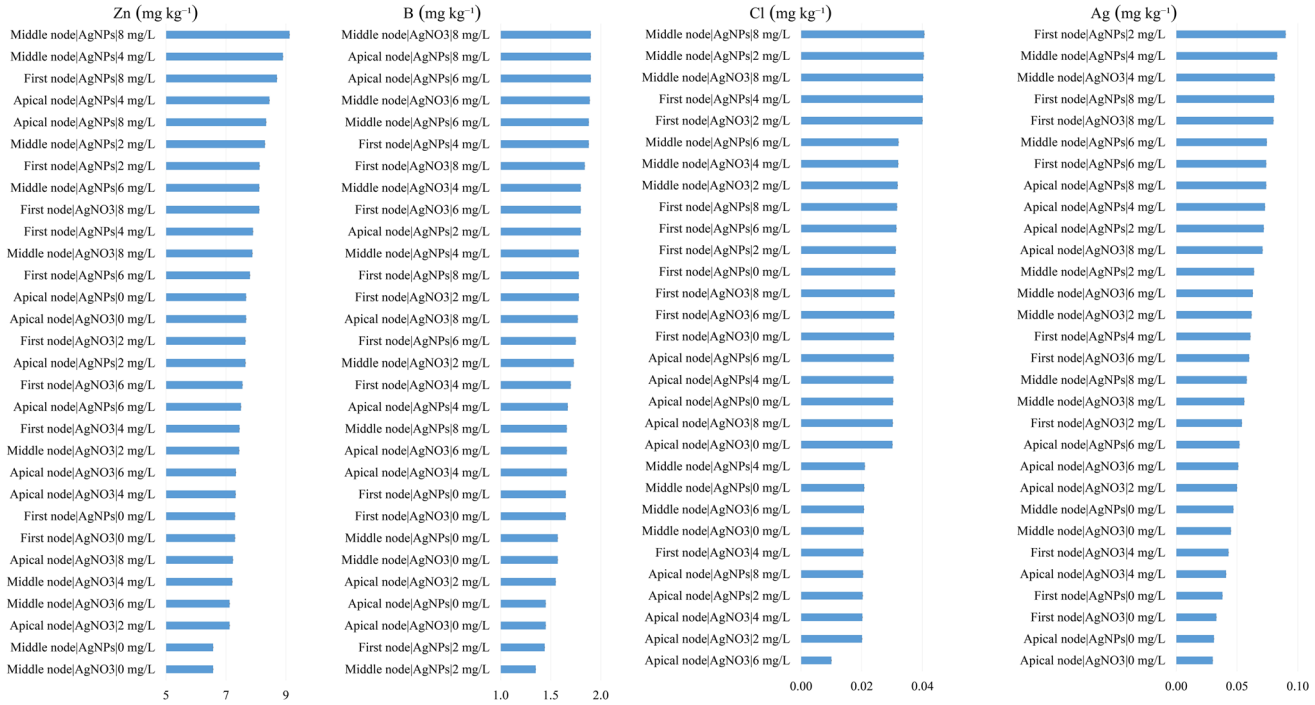

Fig. 9 Three-way interaction effects of explant type, silver source ($AgNO_3$ and Ag-NPs), and Ag concentration on Zn, B, Cl, and Ag accumulation in in vitro cultured explants

weight."it was discovered that the x-axis (F1). which accounts for 77.30% of the variance. has a substantial association with the variables. Higher Ag-NPs concentrations (4 mg L^{-1}, 6 mg L^{-1}, and 8 mg L^{-1}) coupled with apical node and first node explant location boosted shoot development and weight. This was shown by the fact that treatments with the codes S22. S25. S27. S28. and S30 exhibited higher values for shoot length. leaf number. and shoot weight factors. Treatments with the codes S7. S13. S19. S20. S21. S23. s26. and S29 were shown to have positive but weak relationships with callus development. The y-axis (F2) was connected with the variable"callus number."which captured 14.93% of the potential variation.

Figure 11 presents a biplot showing the distribution of treatments (S1 to S30) along the first two principal components. F1 and F2. which together account for 57.38% of the total variance. Ca. Mg. Ag. Na. Mn. and Fe elements were found to be related with the x-axis (F_1). which was shown to capture 42.82 percent of the variation. The treatments that were coded with S8. S11. S12. S13. S15. S19. S24. and S25 had a positive correlation with the elements K. P. B. Ca. Cu. Ag. and Mg. This showed that the nutrient accumulation was higher under more AgNO3 concentrations and explant types. On the other hand. the treatments that were coded with S14. S20. S21. S22. S23. S26. S27. S28. S29. and S30 had a positive correlation with the elements Fe. Mn. Zn. and Cl. This indicated that the nutrient accumulation was higher under more Ag-NPs concentrations and explant types. It was only under conditions of $AgNO_3$ concentrations and explant types that treatments with the codes S2. S4. S5. S7. S9. S10. and S17 had a positive correlation with the element Na. showing that greater levels of Na accumulation were seen.

Figure 12 illustrates a biplot that visualizes the distribution of treatments (S1 to S30) along the first two principal components. F_1 and F_2. which collectively explains 77.92% of the total variance. A significant correlation was found between H_2O_2 and treatments that were classified with S1. S3. S7. S11. S16. and S18. This demonstrated that AgNO3 therapy and various explant types boosted H_2O_2 activity more than other treatments. Treatments that were coded with S9. S10. S12. S13. S15. S19. S21. S26. and S27 were shown to have a positive correlation with SOD and MDA. This finding supported the hypothesis that AgNO3 and Ag-NPs treatments were mostly linked with concentrations of 4 and 6 mg L^{-1}. Both POD and CAT were shown to have a positive correlation with treatments coded with S14. S20. S22. S24. S25. S28. S29. and S30. This finding suggested that Ag-NPs therapy and various explant types tended to boost POD and CAT activity more than other treatments.

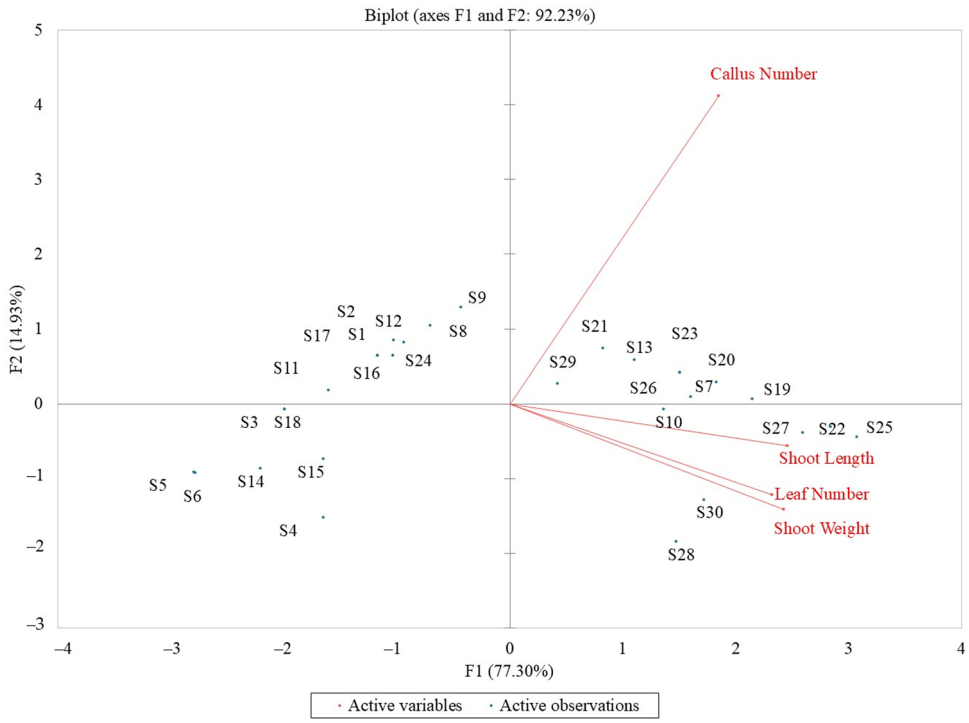

Fig. 10 A two-dimensional graph obtained from PCA of quinoa plant. S1. 0 mg L^{-1} $AgNO_3$+apical node; S2. 0 mg L^{-1} AgNO3+middle node; S3. 0 mg L^{-1} $AgNO_3$+first node; S4. 2 mg L^{-1} $AgNO_3$+apical node; S5. 2 mg L^{-1} $AgNO_3$+middle node; S6. 2 mg L^{-1} $AgNO_3$+first node; S7. 4 mg L^{-1} $AgNO_3$+apical node; S8. 4 mg L^{-1} AgNO3+middle node; S9. 4 mg L^{-1} $AgNO_3$+first node; S10. 6 mg L^{-1} $AgNO_3$+apical node; S11. 6 mg L^{-1} $AgNO_3$+middle node; S12. 6 mg L^{-1} $AgNO_3$+first node; S13. 8 mg L^{-1} $AgNO_3$+apical node; S14. 8 mg L^{-1} $AgNO_3$+middle node; S15. 8 mg L^{-1} $AgNO_3$+first node; S16. 0 mg L^{-1} Ag-NPs+apical node; S17. 0 mg L^{-1} Ag-NPs+middle node; S18. 0 mg L^{-1} Ag-NPs+first node; S19. 2 mg L^{-1} Ag-NPs+apical node; S20. 2 mg L^{-1} Ag-NPs+middle node; S21. 2 mg L^{-1} Ag-NPs+first node; S22. 4 mg L^{-1} Ag-NPs+apical node; S23. 4 mg L^{-1} Ag-NPs+middle node; S24. 4 mg L^{-1} Ag-NPs+first node; S25. 6 mg L^{-1} Ag-NPs+apical node; S26. 6 mg L^{-1} Ag-NPs+middle node; S27. 6 mg L^{-1} Ag-NPs+first node; S28. 8 mg L^{-1} Ag-NPs+apical node; S29. 8 mg L^{-1} Ag-NPs+middle node; S30. 8 mg L^{-1} Ag-NPs+first node

Discussion

Due to the unique properties of nanoparticles, plant interactions with them cause a wide range of morphological and physiological changes. Many variables affect nanoparticle performance, including their chemical composition, size, surface area, reactivity and, most importantly, dosage (Khodakovskaya et al. 2012). It should be noted that the efficacy of nanoparticles differs among plant species and is concentration dependent. Incorporation of $AgNO_3$ into tissue culture media greatly enhanced the regeneration ability of monocotyledonous and dicotyledonous plants. Exactly how $AgNO_3$ affects plants is still unknown. However, there is little evidence that it plays a role in ethylene-sensing circuits. Due to its water solubility and lack of phytotoxicity at effective concentration, $AgNO_3$ has been used as a countermeasure against ethylene in tissue culture research (Kumar et al. 2009). Recent studies have shown that different plant species can benefit from the introduction of silver nanoparticles (Ag-NPs) such as $AgNO_3$ into tissue culture media. One possible explanation for the beneficial effects of Ag-NPs on in vitro procedures such as micropropagation, regeneration and callus induction are that they are predicted to limit ethylene synthesis in the growth medium.

This study revealed that shoot length, callus number, leaf number and shoot weight varied depending on the type of treatment ($AgNO_3$ and Ag-NPs) and the amount of concentration applied. The results of the analysis of variance show that treatment type, concentration and explant type all had statistically significant effects on plant growth parameters ($p \leq 0.001$). It reveals that all three factors (type of treatment, concentration and explant type) play critical roles in plant growth and different combinations cause significant changes in growth parameters. Ag-NPs treatment achieved higher values than $AgNO_3$ treatment in all growth parameters. For example, shoot length (2.820 cm), callus number (8.027 number), leaf number (13.760 number) and shoot weight (3.673 g) were higher with Ag-NPs. This may indicate that the growth-promoting effect of Ag-NPs is greater than that of $AgNO_3$.

Looking at the effect of different concentrations (0.5, 2, 4, 6 and 8 mg L^{-1}), generally higher concentrations resulted in increased growth parameters. However, the highest growth

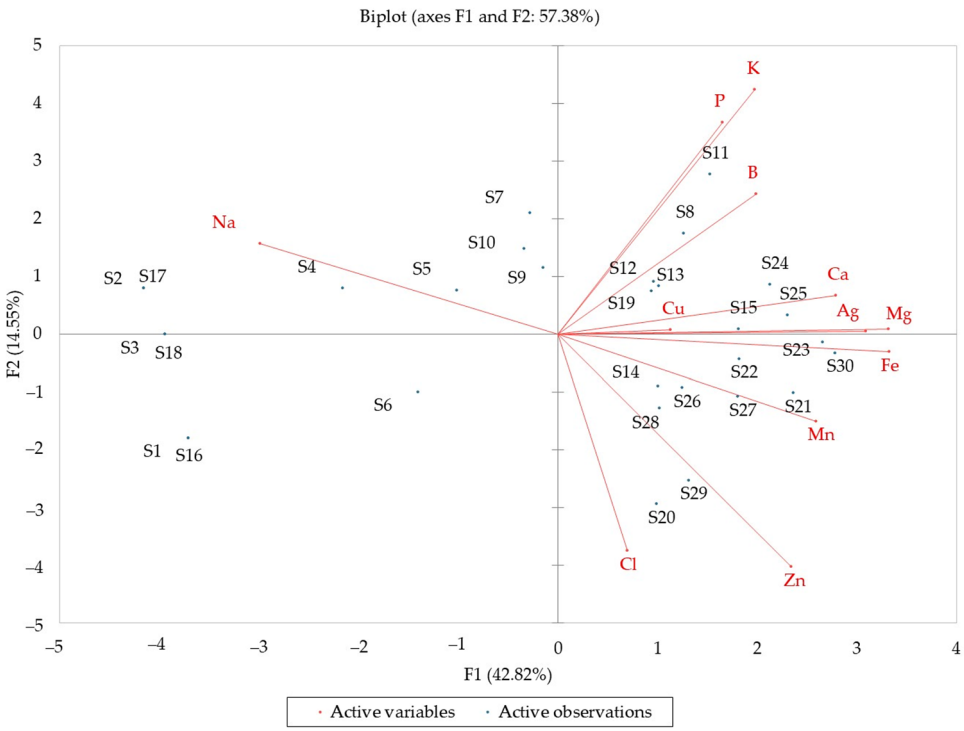

Fig. 11 A two-dimensional graph obtained from PCA of nutrients. S1. 0 mg L^{-1} $AgNO_3$ + apical node; S2. 0 mg L^{-1} AgNO3 + middle node; S3. 0 mg L^{-1} $AgNO_3$ + first node; S4. 2 mg L^{-1} $AgNO_3$ + apical node; S5. 2 mg L^{-1} $AgNO_3$ + middle node; S6. 2 mg L^{-1} $AgNO_3$ + first node; S7. 4 mg L^{-1} $AgNO_3$ + apical node; S8. 4 mg L^{-1} $AgNO_3$ + middle node; S9. 4 mg L^{-1} $AgNO_3$ + first node; S10. 6 mg L^{-1} $AgNO_3$ + apical node; S11. 6 mg L^{-1} $AgNO_3$ + middle node; S12. 6 mg L^{-1} $AgNO_3$ + first node; S13. 8 mg L^{-1} $AgNO_3$ + apical node; S14. 8 mg L^{-1} $AgNO_3$ + middle node; S15. 8 mg L^{-1} $AgNO_3$ + first node; S16. 0 mg L^{-1} Ag-NPs + apical node; S17. 0 mg L^{-1} Ag-NPs + middle node; S18. 0 mg L^{-1} Ag-NPs + first node; S19. 2 mg L^{-1} Ag-NPs + apical node; S20. 2 mg L^{-1} Ag-NPs + middle node; S21. 2 mg L^{-1} Ag-NPs + first node; S22. 4 mg L^{-1} Ag-NPs + apical node; S23. 4 mg L^{-1} Ag-NPs + middle node; S24. 4 mg L^{-1} Ag-NPs + first node; S25. 6 mg L^{-1} Ag-NPs + apical node; S26. 6 mg L^{-1} Ag-NPs + middle node; S27. 6 mg L^{-1} Ag-NPs + first node; S28. 8 mg L^{-1} Ag-NPs + apical node; S29. 8 mg L^{-1} Ag-NPs + middle node; S30. 8 mg L^{-1} Ag-NPs + first node

parameters were generally obtained at 6 mg mg L^{-1} concentration (e.g. shoot length 2.803 cm, callus number 8.233, leaf number 13.800 and shoot weight 3.632 g). These results suggest that the optimum concentration may be around 6 mg L^{-1}, while higher concentrations (8 mg mg L^{-1}) may cause a decrease in growth parameters. Among the explant types, apical explants had the highest values (shoot length 2.502 cm, callus number 7620, leaf number 18.180 and shoot weight 3.352 g). This may indicate that apical tissues have more growth promoting effects than other explant types. The gaseous components within the tissue culture system have a significant influence on the processes responsible for the growth and development of plants. Some studies have shown that ethylene can inhibit the development of somatic embryos and shoot primordia in callus cultures (Wu et al. 2006). Evidence from plant tissue cultures of many species proves the possible advantages of $AgNO_3$ competing with ethylene binding sites. There is evidence that silver nitrate can promote somatic embryogenesis; this is particularly true in cereals. Furthermore, scanning electron microscopy (SEM) analysis revealed that plants exposed to Ag-NPs did not show any significant deleterious effects (Krishnaraj et al. 2012).

The study analyzed changes in antioxidant enzyme activities (CAT, POD, SOD) and malondialdehyde (MDA) levels, an indicator of lipid peroxidation, associated with the defense mechanisms of plants, while also assessing H_2O_2 levels as a marker of cellular stress. Antioxidant enzymes such as CAT, POD, and SOD indicate plant defense responses to stress conditions (Rajput et al. 2021). Treatment with silver nitrate and silver nanoparticles increased the activity of these enzymes. This increase suggests that the plant produces more ROS in a stressful environment against silver ions and activates defense mechanisms against these species. In particular, the highest CAT and SOD activities in both $AgNO_3$ and Ag-NPs treatment were observed at medium–high concentration of 4 mg L^{-1} and 6 mg L^{-1}, respectively, suggesting that these concentrations were the concentrations that triggered the enzymatic defense the most. However, the lower activity at lower concentrations may suggest that the plant's ability to cope with ROS is not yet fully activated under these conditions. Increases in MDA

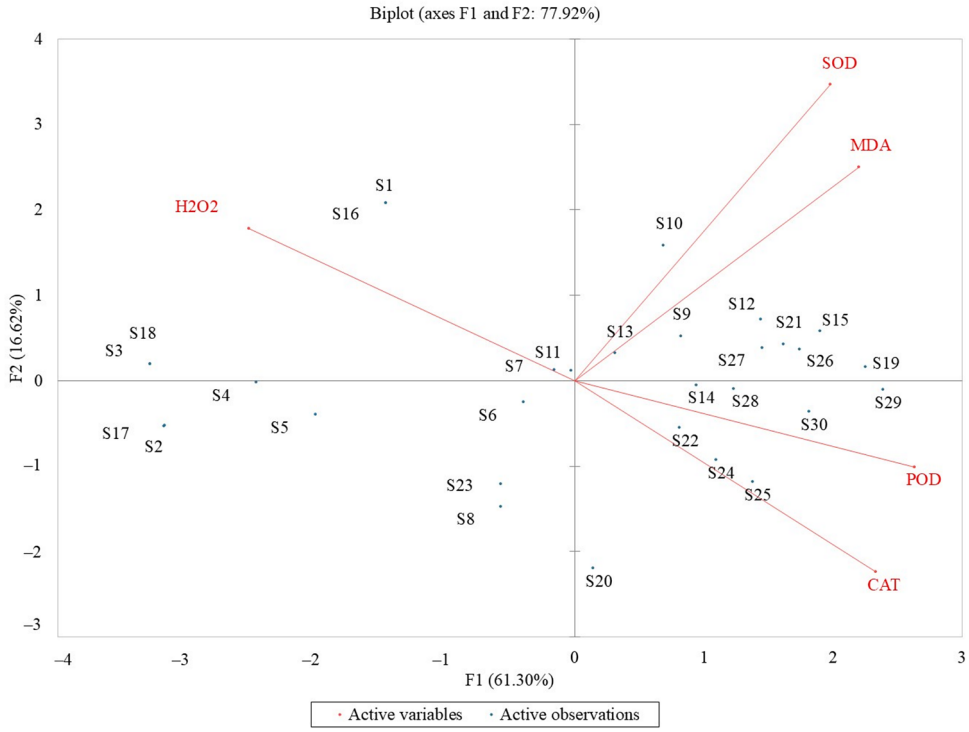

Fig. 12 Two-dimensional graph obtained from PCA of Biochemical measurements. S1. 0 mg L^{-1} $AgNO_3$ + apical node; S2. 0 mg L^{-1} $AgNO_3$ + middle node; S3. 0 mg L^{-1} $AgNO_3$ + first node; S4. 2 mg L^{-1} $AgNO_3$ + apical node; S5. 2 mg L^{-1} $AgNO_3$ + middle node; S6. 2 mg L^{-1} $AgNO_3$ + first node; S7. 4 mg L^{-1} $AgNO_3$ + apical node; S8. 4 mg L^{-1} $AgNO_3$ + middle node; S9. 4 mg L^{-1} $AgNO_3$ + first node; S10. 6 mg L^{-1} $AgNO_3$ + apical node; S11. 6 mg L^{-1} $AgNO_3$ + middle node; S12. 6 mg L^{-1} $AgNO_3$ + first node; S13. 8 mg L^{-1} $AgNO_3$ + apical node; S14. 8 mg L^{-1} $AgNO_3$ + middle node; S15. 8 mg l^{-1} $AgNO_3$ + first node; S16. 0 mg L^{-1} Ag-NPs + apical node; S17. 0 mg L^{-1} Ag-NPs + middle node; S18. 0 mg L^{-1} Ag-NPs + first node; S19. 2 mg L^{-1} Ag-NPs + apical node; S20. 2 mg L^{-1} Ag-NPs + middle node; S21. 2 mg L^{-1} Ag-NPs + first node; S22. 4 mg L^{-1} Ag-NPs + apical node; S23. 4 mg L^{-1} Ag-NPs + middle node; S24. 4 mg L^{-1} Ag-NPs + first node; S25. 6 mg L^{-1} Ag-NPs + apical node; S26. 6 mg L^{-1} Ag-NPs + middle node; S27. 6 mg L^{-1} Ag-NPs + first node; S28. 8 mg L^{-1} Ag-NPs + apical node; S29. 8 mg L^{-1} Ag-NPs + middle node; S30. 8 mg L^{-1} Ag-NPs + first node

levels indicate peroxidative damage of cell membranes. In this study, an increase in MDA levels was observed during both $AgNO_3$ and Ag-NPs treatments. This may indicate an increase in ROS production and consequently cellular damage in the plant. However, the lowest MDA levels were found at lower concentration of $AgNO_3$ and Ag-NPs, indicating that these concentrations were milder in terms of oxidative stress on the plant. In particular, the observation of the lowest MDA levels at concentration of 0.5 mg L^{-1} suggests that lower concentration causes less damage to the plant and that defense mechanisms function adequately at these concentrations. H_2O_2 is an important indicator of cellular stress and ROS accumulation (Kuźniak and Urbanek 2000; Rojkind et al. 2002). This is an interesting finding, because generally higher concentrations are associated with greater stress and H_2O_2 production (Considine and Foyer 2021; Jahan et al. 2023). A possible explanation for this may be that above a certain dose in the plant, ROS scavenging mechanisms are activated and H_2O_2 is eliminated more effectively. The lowest H_2O_2 levels were observed at high concentration (8 mg L^{-1}). This suggests that high concentration may prevent H_2O_2 accumulation by excessively stimulating ROS scavenging enzyme activities. Silver nitrate and silver nanoparticles increased oxidative stress in quinoa plants, resulting in an increase in antioxidant enzyme activities. This enzymatic increase indicates that the plant tries to stabilize oxidative stress. The decrease in H_2O_2 levels suggests that ROS scavenging mechanisms become more efficient at higher concentration. This may indicate that the plant is able to scavenge ROS more effectively above a certain threshold dose or that ROS production is less stimulated above this concentration. It is noteworthy that in both $AgNO_3$ and Ag-NPs applications, medium–high concentration (4–6 mg L^{-1}) generally led to maximum increase in nutrients, but some elements decreased at the highest dose of 8 mg L^{-1}. This may suggest that excessive Ag concentrations may suppress plant metabolism, leading to barriers in nutrient uptake. Since high concentration is known to have toxic effects on plants, the impairment in nutrient uptake may be attributed to this toxicity (Considine and Foyer 2021; Jahan et al. 2023).

In the study, when the effects of Ag-NO_3 and Ag-NPs applications on the nutrient status of the plants were

examined, the concentrations of P, K, Mg, Fe, Cu, Mn, Zn, Cl, and Ag elements generally increased with increasing concentration of AgNO3 and Ag-NPs in both treatments. This indicates that increased silver ions can affect metabolic activities and the uptake of mineral elements in plant cells. In particular, the increase of macro elements such as P and K suggests that plants try to regulate cellular energy metabolism and ion balance, thus adapting to high Ag ion concentrations (Considine and Foyer 2021; Jahan et al. 2023). Na decreased with increasing concentrations in both $AgNO_3$ and Ag-NPs treatments, while Ca levels decreased above 8 mg L^{-1} for $AgNO_3$ and 6 mg L^{-1} for Ag-NPs. Decreased sodium uptake suggests that Ag may have a negative effect on ion balance in the plant. A decrease in Na may indicate a disturbance of osmoregulation or a problem with ion transport in the plant. A decrease in calcium may lead to weakening of the structural integrity of the plant, especially as an element that plays an important role in maintaining cell walls and membrane stability. This may indicate that high Ag concentration impairs ion transport in the plant and causes changes in the permeability of cellular membranes (Kumari and Rathore 2020; Liu et al. 2024). An increase in Mg and P may indicate that enzymatic reactions supporting the metabolic processes of the plant are accelerated and that these elements, which play an important role in ATP synthesis, are more utilized in response to increased Ag concentrations. The increase of microelements such as Fe, Cu, Mn and Zn indicates that the plant requires more antioxidant enzyme activities to cope with increased Ag ion stress and that these microelements play critical roles in defense mechanisms. These elements provide plant protection against increased ROS (reactive oxygen species) stress, especially since they act as cofactors for antioxidative enzymes (Foyer and Shigeoka 2011). The decrease in Na level with increasing concentration of $AgNO_3$ and Ag-NPs is an important factor that directly affects the ion balance and osmotic regulation of plants. The decrease in Na indicates that Ag ions may have an inhibitory effect on ion transport or ion channels in plants. At the same time, the decrease in Ca levels suggests that the membrane stability of the plant cell is impaired, and this may have negative effects on the plant under stress conditions (Kumar et al. 2023). $AgNO_3$ and Ag-NPs treatments caused changes in important nutrients in quinoa plants. In general, an increase in important macro elements such as phosphorus, potassium and magnesium were observed, while a decrease was observed in elements affecting ion balance such as sodium and calcium. This is important for understanding the strategies of plants to cope with increased Ag ions and the negative effects of silver onion transport. It is seen that silver applications, especially at high concentrations, may cause toxic effects on the plant and this may have negative consequences on plant growth and nutrient uptake (Foyer and Shigeoka 2011; Kumari and Rathore 2020). These results provide important information for the use of nanoparticles in agricultural production and for understanding the effects of environmental silver pollution on plants. It should be noted that Ag-NPs have potential benefits in agriculture, but also a risk factor that requires careful use. It is important to understand the biochemical effects of environmental stressors on plants and to develop potential stress tolerance strategies. Further research is needed to evaluate the effects of silver nanoparticles on plant health.

Conclusions

This study highlights the complex interactions between silver-based compounds, particularly Ag-NO_3 and Ag-NPs, and plant physiological processes. The findings demonstrate that both Ag-NO_3 and Ag-NPs influence essential plant growth parameters such as shoot length, callus formation, leaf number, and shoot weight, with Ag-NPs generally showing more pronounced positive effects. The observed enhancement in antioxidant enzyme activities and the rise in MDA levels indicate that silver ions trigger oxidative stress in plants, leading to the activation of defense mechanisms. At medium to high concentrations (4–6 mg L^{-1}), plants exhibited the highest enzymatic activity, suggesting a dose-dependent response to mitigate ROS stress. The increase in macro elements like P, K, and Mg implies that plants attempt to adapt to high Ag ion stress by regulating cellular energy metabolism and ion balance. However, the decrease in Na and Ca levels at higher concentration indicates potential disruptions in ion transport and membrane stability, which could impair osmotic regulation and structural integrity. While Ag-NPs offer promising applications in enhancing tissue culture processes and plant regeneration, the data also highlights the potential risks of toxicity at higher concentrations. These findings underscore the need for further research to optimize the use of silver nanoparticles in agriculture while minimizing environmental and biological risks. Understanding the delicate balance between beneficial and harmful effects of Ag-based compounds is crucial for future applications in sustainable agriculture and environmental management.

Acknowledgements We thank the anonymous reviewers and editors for their constructive comments on this manuscript.

Author contributions Conceptualization, A.T. and K.H.; methodology, A.T., K.H. and E.İ.; software, B.E., F.D., and M.İ.I.; validation, A.T., S.Ç. and A.G.; formal analysis, B.E., F.D., A.T. and K.H.; investigation, K.H. and A.T.; resources, K.H.; data curation, A.T., A.G. and S.Ç.; writing—original draft preparation, A.T., B.E., F.D., and K.H.; writing—review and editing, A.T., H.A.H. and K.H.; visualization, K.H. and A.T.; supervision, K.H.; project administration, K.H.; fund-

ing acquisition, K.H. All authors have read and agreed to the published version of the manuscript.

Data availability All data supporting the conclusions of this article are included in this article.

Declarations

Competing interests The authors declare that they have no conflict of interest.

References

Bello-Bello JJ, Spinoso-Castillo JL, Arano-Avalos S, Martínez-Estrada E, Arellano-García ME, Pestryakov A, Toledano-Magaña Y, García-Ramos JC, Bogdanchikova N (2018) Cytotoxic, genotoxic, and polymorphism effects on *Vanilla planifolia* Jacks ex Andrews after long-term exposure to Argovit® silver nanoparticles. Nanomaterials 8(10):754. https://doi.org/10.3390/nano8100754

Bhojwani SS, Dantu PK (2013) Micropropagation Plant tissue culture: An introductory text. Springer 245:274. https://doi.org/10.1007/978-81-322-1026-9_17

Biddington N (1992) The influence of ethylene in plant tissue culture. Plant Growth Regul 11:173–187. https://doi.org/10.1007/BF00024072

Çiçek S (2022) Cytotoxicity of silver nanoparticles obtained from Eruca vesicaria on rainbow trout gonad cell line-2 (RTG-2). Gümüşhane Üniversitesi Fen Bilimleri Dergisi. 12(4):1093–1101. https://doi.org/10.17714/gumusfenbil.1104370

Çığ F, Toprak ÇC, Erden Z (2024) Nanotechnology and the use of nanoparticles and its effect on wheat growing. Muş Alparslan University Journal of Agriculture and Nature 4(1):23–29. https://doi.org/10.59359/maujan.1344423

Considine MJ, Foyer CH (2021) Stress effects on the reactive oxygen species-dependent regulation of plant growth and development. J Exp Bot 72(16):5795–5806. https://doi.org/10.1093/jxb/erab265

Cristea T, Leonte C, Brezeanu C, Brezeanu M, Ambarus S, Calin M, Prisecaru M (2012) Effect of AgNO3 on androgenesis of *Brassica oleracea* L. anthers cultivated in vitro. Afr J Biotechnol 11(73):13788–13795. https://doi.org/10.5897/AJB12.2157

Dosad S, Chawla HS (2015) *In vitro* plant regeneration from mature seeds of finger millet (*Eleusine coracana*) through somatic embryogenesis. Indian J Plant Physiol 20:360–367. https://doi.org/10.1007/s40502-015-0191-2

Foyer CH, Shigeoka S (2011) Understanding oxidative stress and antioxidant functions to enhance photosynthesis. Plant Physiol 155(1):93–100. https://doi.org/10.1104/pp.110.166181

Ghormade V, Deshpande MV, Paknikar KM (2011) Perspectives for nano-biotechnology enabled protection and nutrition of plants. Biotechnol Adv 29(6):792–803. https://doi.org/10.1016/j.biotechadv.2011.06.007

Haverkamp R, Marshall A (2009) The mechanism of metal nanoparticle formation in plants: limits on accumulation. J Nanopart Res 11:1453–1463. https://doi.org/10.1007/s11051-008-9533-6

Hesami M, Daneshvar MH (2016) Development of a regeneration protocol through indirect organogenesis in *Chenopodium quinoa* Willd. Indo Am J Agric Vet Sci 4(2):25–32

Jahan A, Khan MMA, Ahmad B, Ahmed KBM, Pandey RP, Gulfishan M (2023) Hydrogen peroxide: regulator of plant development and abiotic stress response Reactive Oxygen Species: Prospects in Plant Metabolism. Springer 213:228. https://doi.org/10.1007/978-981-19-9794-5_12

Ji B, Xuan L, Zhang Y, Mu W, Paek K-Y, Park S-Y, Wang J, Gao W (2023) Application of data modeling, instrument engineering and nanomaterials in selected medid the scientific recinal plant tissue culture. Plants 12(7):1505. https://doi.org/10.3390/plants12071505

Jiménez VM (2001) Regulation of *in vitro* somatic embryogenesis with emphasis on to the role of endogenous hormones. Rev Bras Fisiol Veg 13:196–223. https://doi.org/10.1590/S0103-31312001000200008

Kaysım MG, Kumlay AM, Haliloglu K, Türkoğlu A, Piekutowska M, Nadaroğlu H, Alayli A, Niedbała G (2024) Physiological and antioxidative effects of Strontium oxide nanoparticles on wheat. Agronomy 14(4):770. https://doi.org/10.3390/agronomy14040770

Khan S, Zahoor M, Khan RS, Ikram M, Islam NU (2023) The impact of silver nanoparticles on the growth of plants: the agriculture applications. Heliyon. https://doi.org/10.1016/j.heliyon.2023.e16928

Khodakovskaya MV, De Silva K, Biris AS, Dervishi E, Villagarcia H (2012) Carbon nanotubes induce growth enhancement of tobacco cells. ACS Nano 6(3):2128–2135. https://doi.org/10.1021/nn204643g

Koçak R, Okcu M, Haliloğlu K, Türkoğlu A, Pour-Aboughadareh A, Jamshidi B, Janda T, Alaylı A, Nadaroğlu H (2023) Magnesium oxide nanoparticles: an influential element in cowpea (*Vigna unguiculata* L. Walp.) tissue culture. Agronomy 13(6):1646. https://doi.org/10.3390/agronomy13061646

Krishnaraj C, Ramachandran R, Mohan K, Kalaichelvan P (2012) Optimization for rapid synthesis of silver nanoparticles and its effect on phytopathogenic fungi. Spectrochim Acta A Mol Biomol Spectrosc 93:95–99. https://doi.org/10.1016/j.saa.2012.03.002

Kulus D, Tymoszuk A (2021) Gold nanoparticles affect the cryopreservation efficiency of *in vitro*-derived shoot tips of bleeding heart. Plant Cell, Tissue and Organ Culture (PCTOC) 146(2):297–311. https://doi.org/10.1007/s11240-021-02069-4

Kumar V, Parvatam G, Ravishankar GA (2009) AgNO3: a potential regulator of ethylene activity and plant growth modulator. Electron J Biotechnol 12(2):8–9

Kumar S, Masurkar P, Sravani B, Bag D, Sharma KR, Singh P, Korra T, Meena M, Swapnil P, Rajput VD (2023) A review on phytotoxicity and defense mechanism of silver nanoparticles (AgNPs) on plants. J Nanopart Res 25(4):54. https://doi.org/10.1007/s11051-023-05708-3

Kumari J, Rathore MS (2020) Na+/K+-ATPase a primary membrane transporter: an overview and recent advances with special reference to algae. J Membr Biol 253(3):191–204. https://doi.org/10.1007/s00232-020-00119-0

Kuźniak E, Urbanek H (2000) The involvement of hydrogen peroxide in plant responses to stresses. Acta Physiol Plant 22:195–203. https://doi.org/10.1007/s11738-000-0076-4

Lin D, Xing B (2007) Phytotoxicity of nanoparticles: inhibition of seed germination and root growth. Environ Pollut 150(2):243–250. https://doi.org/10.1016/j.envpol.2007.01.016

Liu M, Feng N, Zheng D, Zhang R (2024) Prohexadione calcium and gibberellin improve osmoregulation, antioxidant response and ion homeostasis to alleviate NaCl stress in rice seedlings. Agronomy 14(6):1318. https://doi.org/10.3390/agronomy14061318

Mabotja M, Gerrano A, Venter S, du Plooy C, Kudanga T, Amoo S (2021) Nutritional variability in 42 cultivars of spineless cactus pear cladodes for crop improvement. S Afr J Bot 142:140–148. https://doi.org/10.1016/j.sajb.2021.06.022

Mathew M, Philip V (2003) Somatic embryogenesis versus zygotic embryogenesis in *Ensete superbum*. Plant Cell Tissue Organ Cult 72:267–275. https://doi.org/10.1023/A:1022311126043

Murashige T, Skoog F (1962) A revised medium for rapid growth and bio assays with tobacco tissue cultures. Physiol Plant. https://doi.org/10.1111/j.1399-3054.1962.tb08052.x

Parzymies M (2021) Nano-silver particles reduce contaminations in tissue culture but decrease regeneration rate and slows down growth and development of *Aldrovanda vesiculosa* explants. Appl Sci 11(8):3653. https://doi.org/10.3390/app11083653

Pasternak TP, Steinmacher D (2024) Plant growth regulation in cell and tissue culture *in vitro*. Plants 13(2):327. https://doi.org/10.3390/plants13020327

Pérez-Caselles C, Alburquerque N, Faize L, Bogdanchikova N, García-Ramos JC, Rodríguez-Hernández AG, Pestryakov A, Burgos L (2022) How to get more silver? Culture media adjustment targeting surge of silver nanoparticle penetration in apricot tissue during *in vitro* micropropagation. Horticulturae 8(10):855. https://doi.org/10.3390/horticulturae8100855

Rabha M, Rout G (2011) An alternative pathway for plant regeneration via somatic embryogenesis of upland rice (*Oryza sativa* cvs. Khandagiri and Vanaprava). J Cell Tissue Res 11(2):2809

Rahmawati M, Mahfud C, Risuleo G, Jadid N (2022) Nanotechnology in plant metabolite improvement and in animal welfare. Appl Sci 12(2):838. https://doi.org/10.3390/app12020838

Rajput VD, Harish SRK, Verma KK, Sharma L, Quiroz-Figueroa FR, Meena M, Gour VS, Minkina T, Sushkova S (2021) Recent developments in enzymatic antioxidant defence mechanism in plants with special reference to abiotic stress. Biol 10(4):267. https://doi.org/10.3390/biology10040267

Reddy PK, Mamatha N, Naik P, Srilatha V, Kumar P (2016) Applications of nanotechnology in agricultural sciences. Andhra Pradesh J Agric Sci 2(1):1–9

Rojkind M, Dominguez-Rosales J-A, Nieto N, Greenwel P (2002) Role of hydrogen peroxide and oxidative stress in healing responses. Cell Mol Life Sci 59:1872–1891. https://doi.org/10.1007/PL00012511

Sahin U, Ekinci M, Ors S, Turan M, Yildiz S, Yildirim E (2018) Effects of individual and combined effects of salinity and drought on physiological, nutritional and biochemical properties of cabbage (*Brassica oleracea* var. *capitata*). Sci Hortic 240:196–204. https://doi.org/10.1016/j.scienta.2018.06.016

Sahrawat AK, Becker D, Lütticke S, Lörz H (2003) Genetic improvement of wheat via alien gene transfer, an assessment. Plant Sci 165(5):1147–1168. https://doi.org/10.1016/S0168-9452(03)00323-6

Tiryaki D, Aydın İ, Atıcı Ö (2019) Psychrotolerant bacteria isolated from the leaf apoplast of cold-adapted wild plants improve the cold resistance of bean (*Phaseolus vulgaris* L.) under low temperature. Cryobiology 86:111–119. https://doi.org/10.1016/j.cryobiol.2018.11.001

Vishwakarma K, Shweta UN, Singh J, Liu S, Singh VP, Prasad SM, Chauhan DK, Tripathi DK, Sharma S (2017) Differential phytotoxic impact of plant mediated silver nanoparticles (AgNPs) and silver nitrate (AgNO3) on *Brassica* sp. Front Plant Sci 8:1501. https://doi.org/10.3389/fpls.2017.01501

Wu J, Song KH, Litzinger T, Lee S-Y, Santoro R, Linevsky M, Colket M, Liscinsky D (2006) Reduction of PAH and soot in premixed ethylene–air flames by addition of ethanol. Combust Flame 144(4):675–687. https://doi.org/10.1016/j.combustflame.2005.08.036

Wu K, Xu C, Li T, Ma H, Gong J, Li X, Sun X, Hu X (2023) Application of nanotechnology in plant genetic engineering. Int J Mol Sci 24(19):14836. https://doi.org/10.3390/ijms241914836

Yan A, Chen Z (2019) Impacts of silver nanoparticles on plants: a focus on the phytotoxicity and underlying mechanism. Int J Mol Sci 20(5):1003. https://doi.org/10.3390/ijms20051003

Yin L, Cheng Y, Espinasse B, Colman BP, Auffan M, Wiesner M, Rose J, Liu J, Bernhardt ES (2011) More than the ions: the effects of silver nanoparticles on *Lolium multiflorum*. Environ Sci Technol 45(6):2360–2367. https://doi.org/10.1021/es103995x

Publisher's Note Springer Nature remains neutral with regard to jurisdictional claims in published maps and institutional affiliations.

Springer Nature or its licensor (e.g. a society or other partner) holds exclusive rights to this article under a publishing agreement with the author(s) or other rightsholder(s); author self-archiving of the accepted manuscript version of this article is solely governed by the terms of such publishing agreement and applicable law.

Authors and Affiliations

Aras Türkoğlu[1] · Kamil Haliloğlu[2] · Ayşegül Kasapoğlu[3] · Damla Kızılkaya[3] · Barış Eren[4] · Fatih Demirel[4] · Muhammet İslam Işık[1] · Emre İlhan[3] · Hossein Abbasi Holasou[5] · Adem Güneş[6]

✉ Aras Türkoğlu
aras.turkoglu@erbakan.edu.tr

✉ Kamil Haliloğlu
kamilh@atauni.edu.tr

Ayşegül Kasapoğlu
aysegul.kasapoglu@erzurum.edu.tr

Damla Kızılkaya
damlakizilkaya25@gmail.com

Barış Eren
baris.eren@igdir.edu.tr

Fatih Demirel
fatih.demirel@igdir.edu.tr

Muhammet İslam Işık
muhammetislam.isik@erbakan.edu.tr

Emre İlhan
emre.ilhan@erzurum.edu.tr

Hossein Abbasi Holasou
hossein.pdf55@gmail.com

Adem Güneş
ademgunes@erciyes.edu.tr

[1] Department of Field Crops, Faculty of Agriculture, Necmettin Erbakan University, 42310 Konya, Turkey

[2] Department of Biology, Faculty of Science, Gazi University, 06170 Ankara, Turkey

[3] Department of Molecular Biology and Genetics, Erzurum Technical University, 25240 Erzurum, Turkey

[4] Department of Agricultural Biotechnology, Faculty of Agriculture, Igdır University, Igdir 76000, Turkey

[5] Department of Plant Breeding and Biotechnology, Faculty of Agriculture, University of Tabriz, Tabriz 5166616471, Iran

[6] Department of Soil Science and Plant Nutrition, Faculty of Agriculture, Erciyes University, Kayseri 38030, Turkey